# Observing the Wind Driven Velocity Structure of the California Current System

Dax Matthews

ATOC 6020
October 13, 2008

# Introduction

- Currents at the ocean surface are caused by many different forces
- At very large scales, many currents are associated with a dynamical balance between a pressure force and the Coriolis force, these currents are called "geostrophic"
- Ageostrophic currents consist of many high frequency currents (such as tides and internal waves)
- At lower frequencies the most dominate ageostrophic current seen in the upper ocean is the directly wind-driven current

# Theory of Wind-driven Ocean Currents

- Modern theory for wind-driven ocean circulation originated from Nasen's qualitative argument explaining why ice in the Artic drift at an angle of 20-40° to the right of the wind (1898)
- He later worked out the balance of forces that must exist when wind pushes icebergs in a rotating Earth

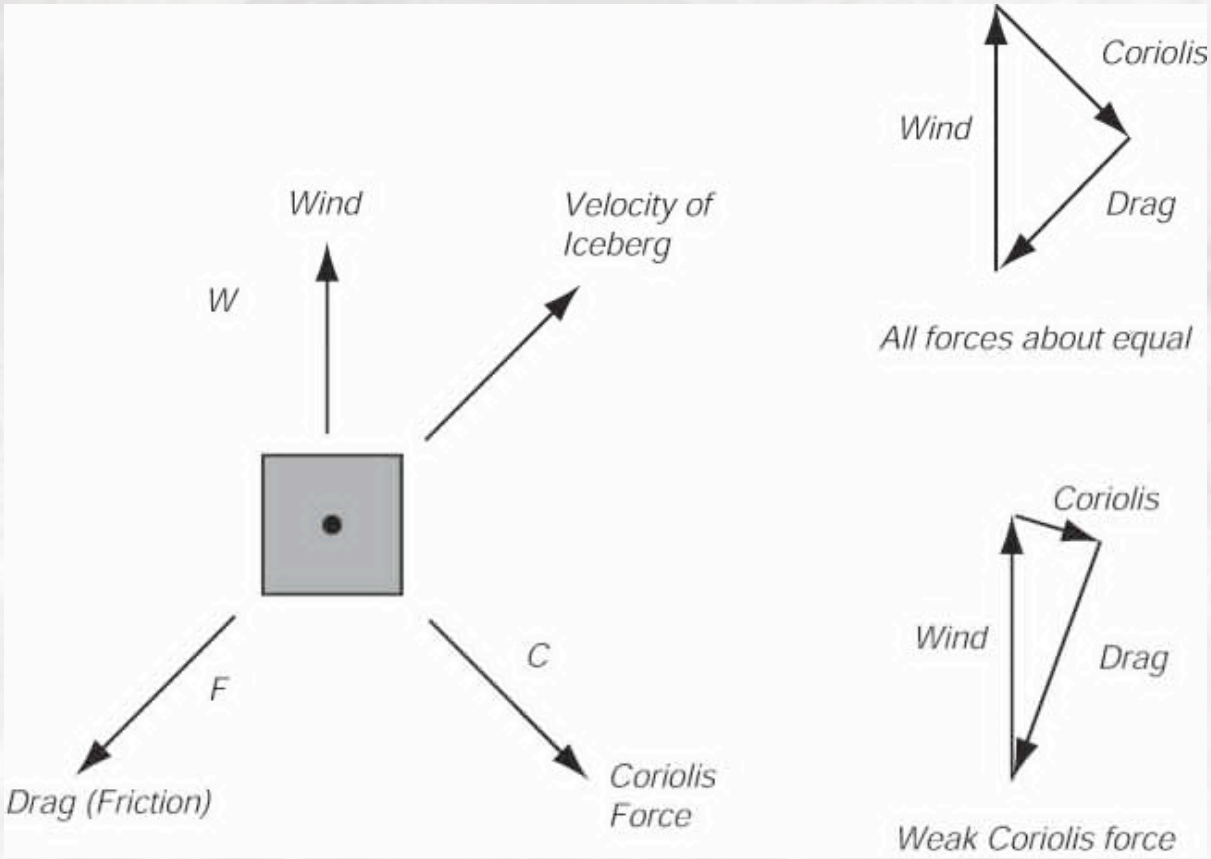

- Nansen's observations led to Ekman's [1905] paper describing the quantitative effect of wind and the Earth's rotation on the upper ocean
- Ekman acknowledged that wind-stress induces vertical mixing in the upper ocean through turbulent processes
- The model for the momentum balance of a steady wind driven current leads to the solutions:

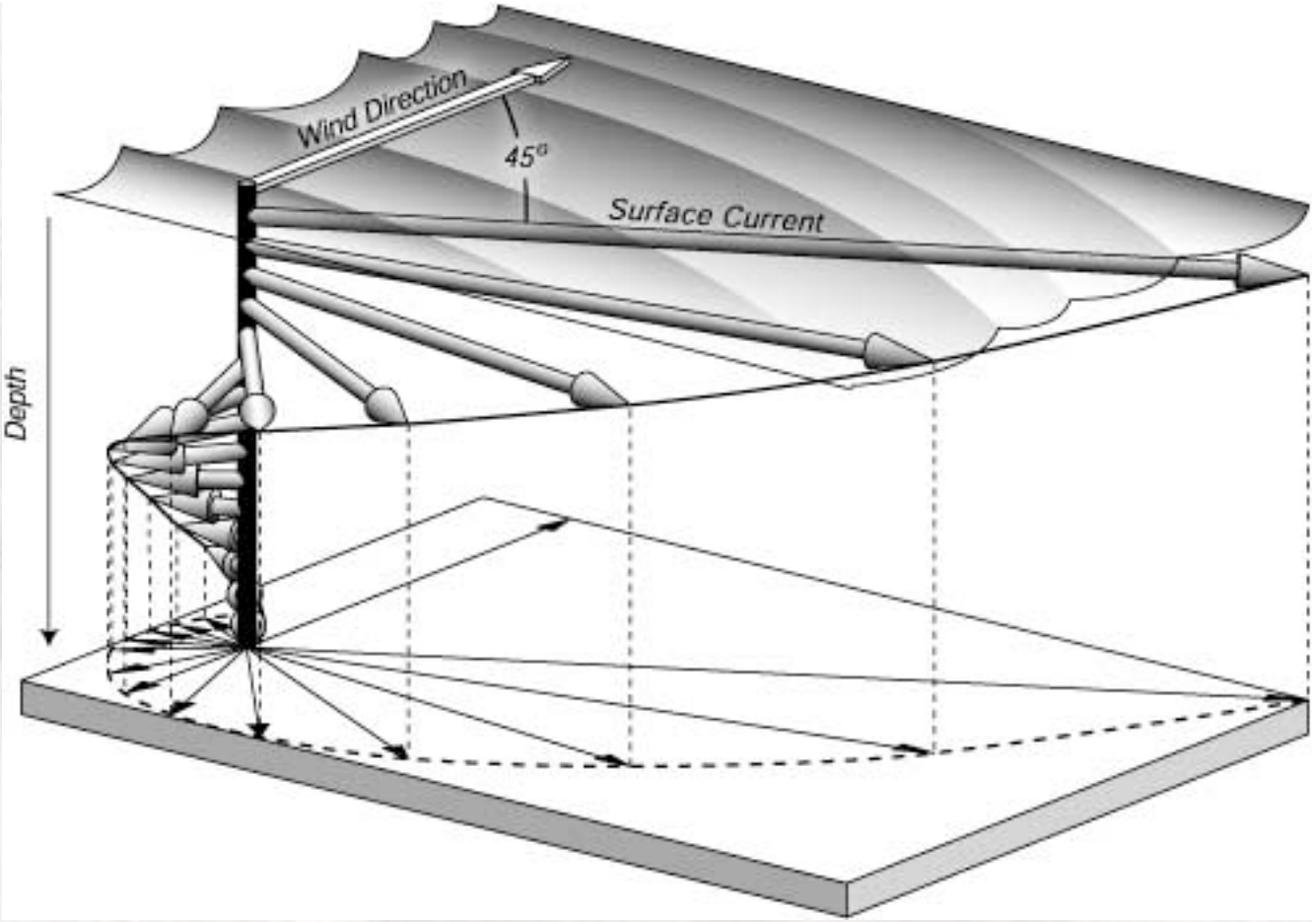


$$u_E = \pm V_0 \cos\left(\frac{\pi}{4} + \frac{\pi}{D_E} z\right) \exp\left(\frac{\pi}{D_E} z\right)$$

$$v_E = V_0 \sin\left(\frac{\pi}{4} + \frac{\pi}{D_E} z\right) \exp\left(\frac{\pi}{D_E} z\right)$$

$V_0$ is the total Ekman surface current
$D_E$ is the effective depth of the Ekman layer
Result: spiral shaped current profile with depth

# Observing Wind-driven Currents

- Several studies have attempted to estimate wind-driven flow using various data sets
- Observational difficulty is one of a low signal-to-noise ratio
- Wind-driven current is masked by geostrophic flow
- Two solutions to this problem:
  - Wind driven flow can be separated from the pressure driven flow by removal of a deep reference current
  - Utilize two data velocity data sets - subtract a measurement of the geostrophic flow from a measurement of the total flow

# Vertical Response

- Wijffels et al. [1993] Estimated wind driven velocity structure using ADCP and CTD data
  - Acoustic Doppler Current Profiler
    - Measures water currents with sound
    - Transmits pings at constant frequency
  - Conductivity Temperature Depth Recorder
    - Estimate density field using equations of state
    - Density used to calculate internal pressure field from which geostrophic currents can be estimated

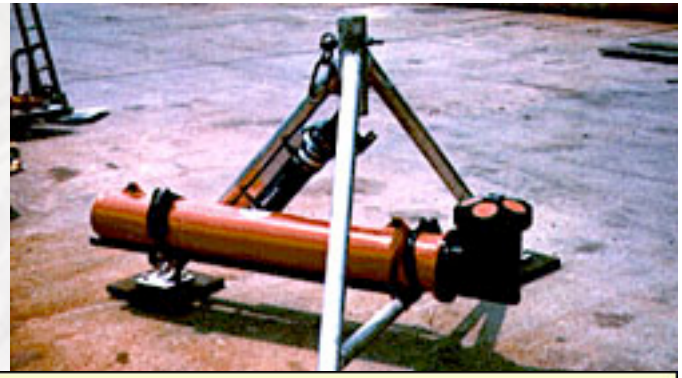

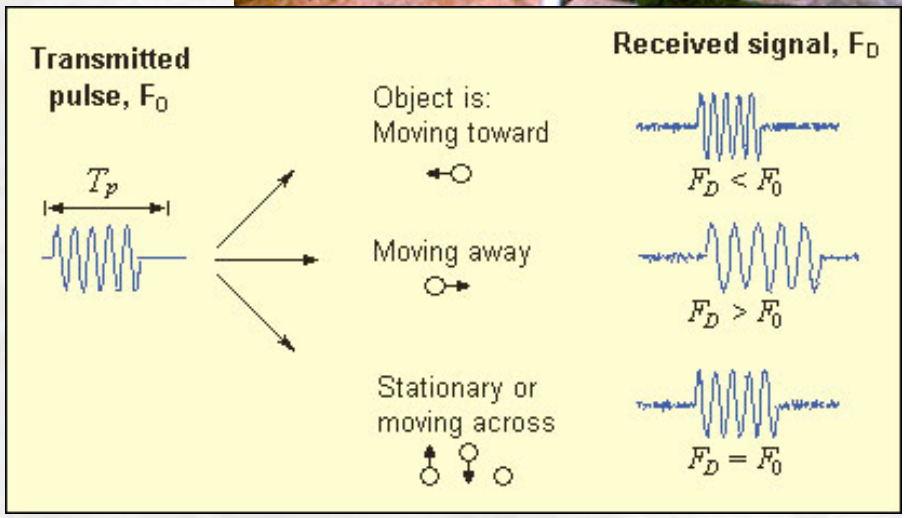


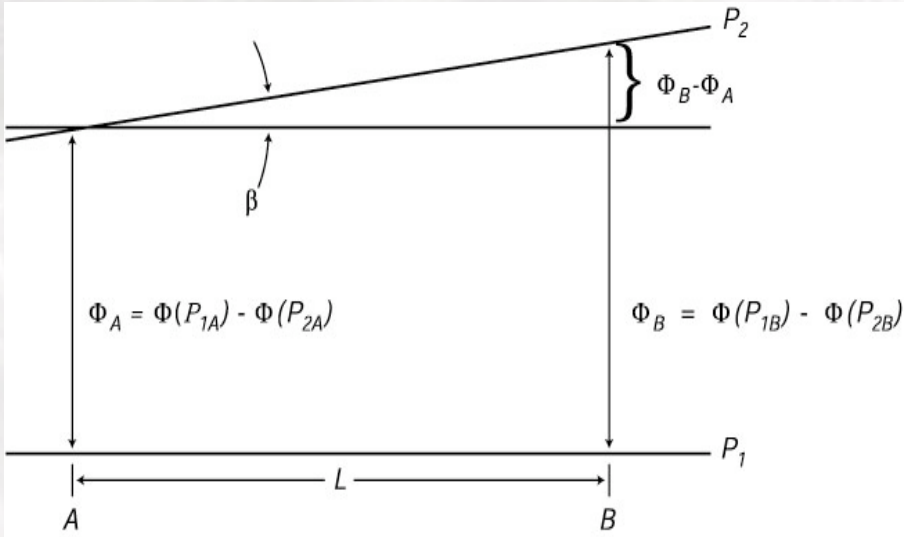

- Chereskin [1995] observed wind-driven flow using moored ADCP and buoy wind observations
  - Wind driven flow separated from total flow by subtraction of a deep reference current
- Mean velocity profiles from both studies show smooth spiral qualitatively similar to theoretical Ekman spiral, however flatter in shape

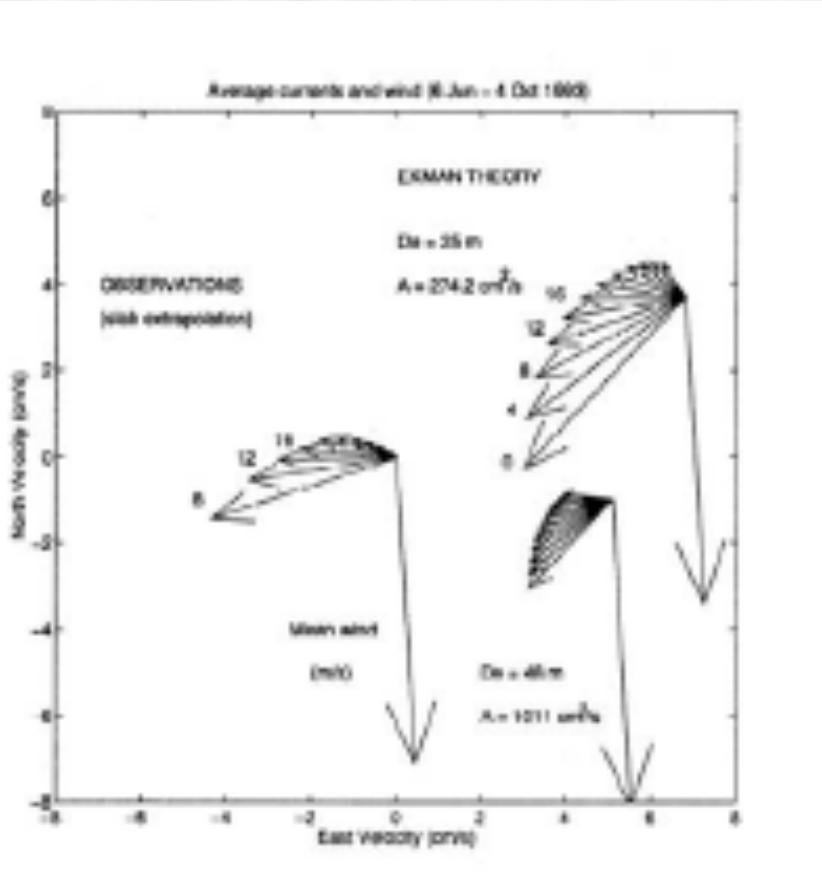

# Horizontal Response

- Ralph and Niiler [1999] use Lagrangian drifters referenced to a hydrographic geostrophic mean to study wind driven currents in the Tropical Pacific
- Satellite tracked drifting buoys
  - Consist of a surface buoy and a subsurface drogue (anchor)
  - Employ holey-sock drogue centered at 15 m
  - TIROS satellites carry the Argos Data Collection and Location System (ADCLS) that allows for global positioning of drifting buoys
  - Measures the total velocity of the current
- Hydrographic climatology
  - Combination of XBT and CTD data
  - Estimates surface dynamic height used to calculate the mean geostrophic current
- Surface winds
  - Ocean Surface Winds Derived from the SSM/I Radiometer

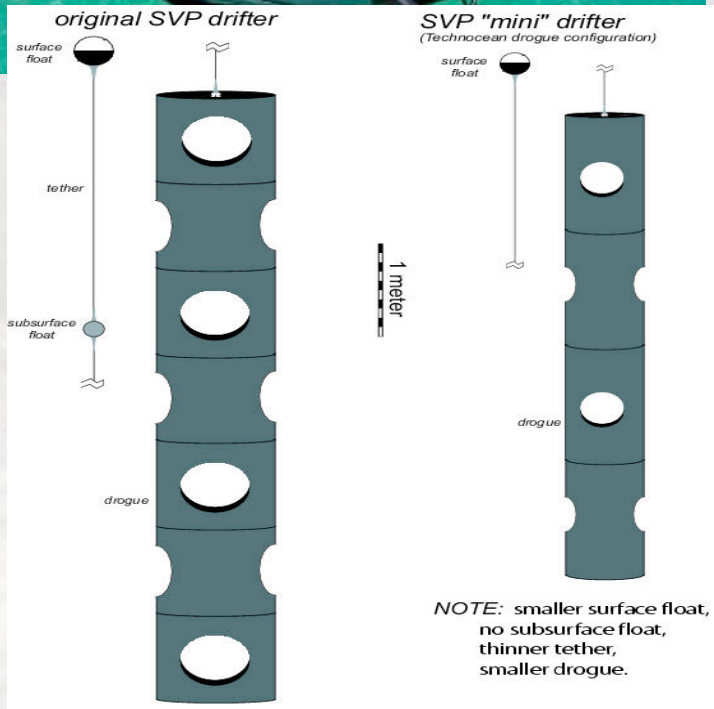

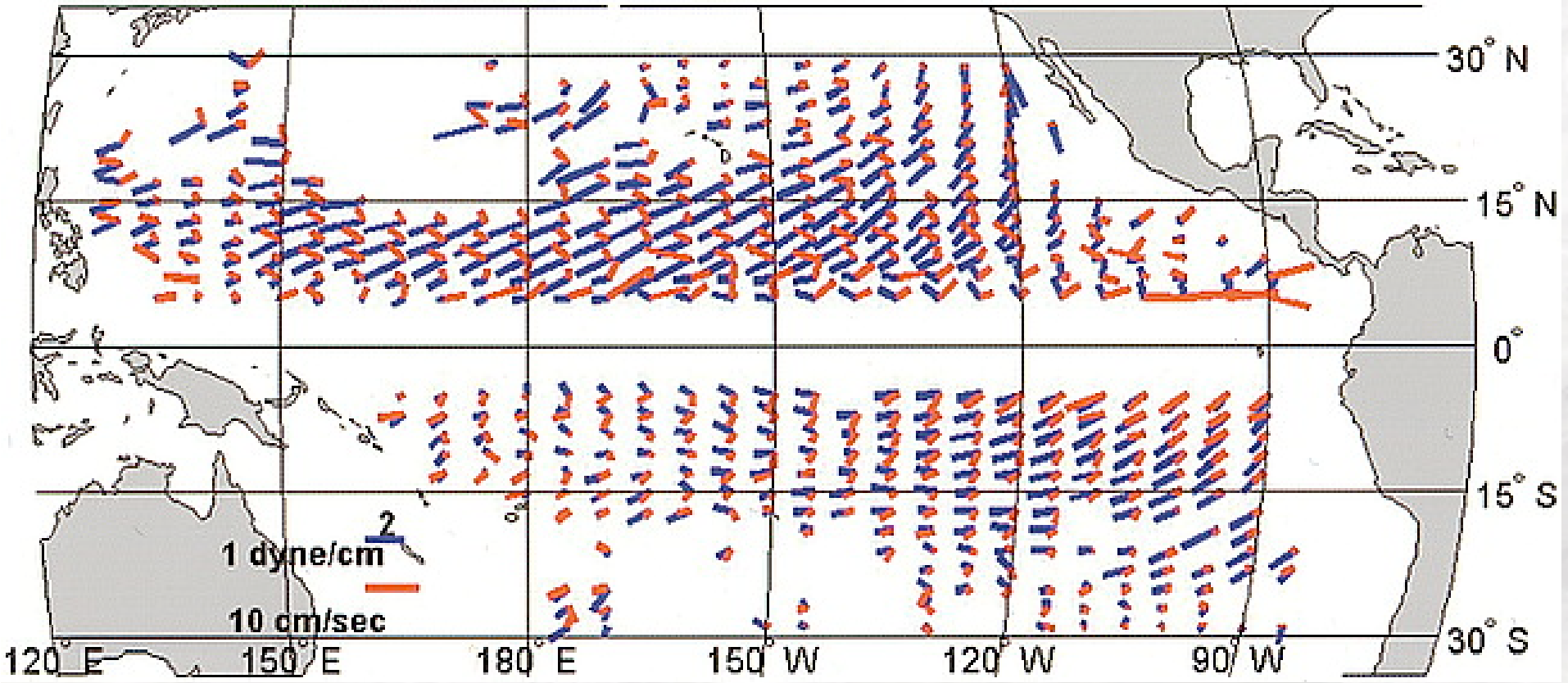


- Mean wind stress and ageostrophic currents
- Distribution shows pattern of wind-driven currents relative to the wind stress deflected to the right(left) in the Northern (Southern) Hemisphere
- Relative strength and rotation is highly variable

- Rio and Hernandez [2003] investigated large-scale response (~5°) of wind-driven currents using surface drifters referenced to satellite altimetry, and ECMWF wind fields
- Satellite altimetry is designed to measure the sea surface by a combination of radar and satellite position data
  - Altimeters measure sea surface height (SSH) variations used to map ocean currents
  - Rio05 Combined Mean Dynamic Topography (MDT) [Rio and Hernandez 2004] is a 7-year (1993-1999) mean profile based on multiple satellite and in-situ data sets
  - Maps of Absolute Dynamic Topography (MADT) are the sum of the sea level anomaly (SLA) and mean dynamic topography (MDT) product
  - Advantage over hydrographic data of being time dependent

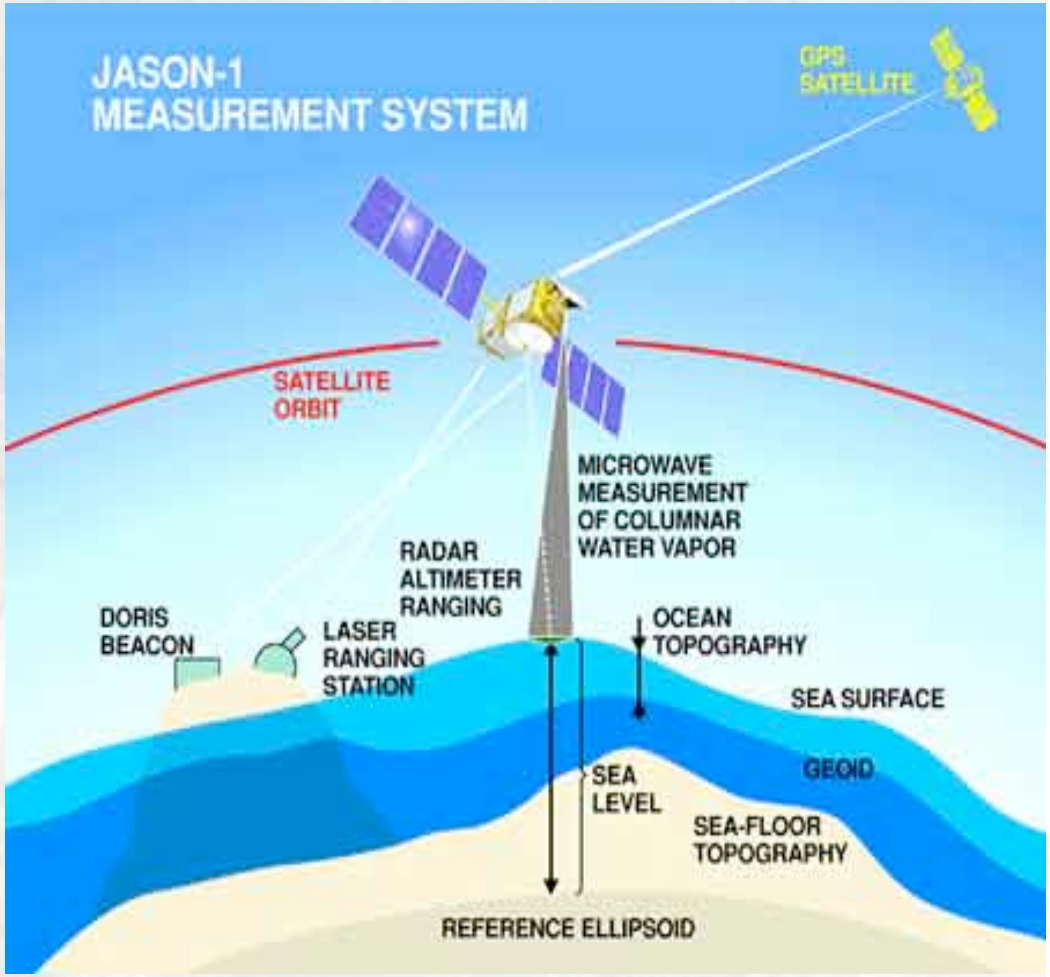

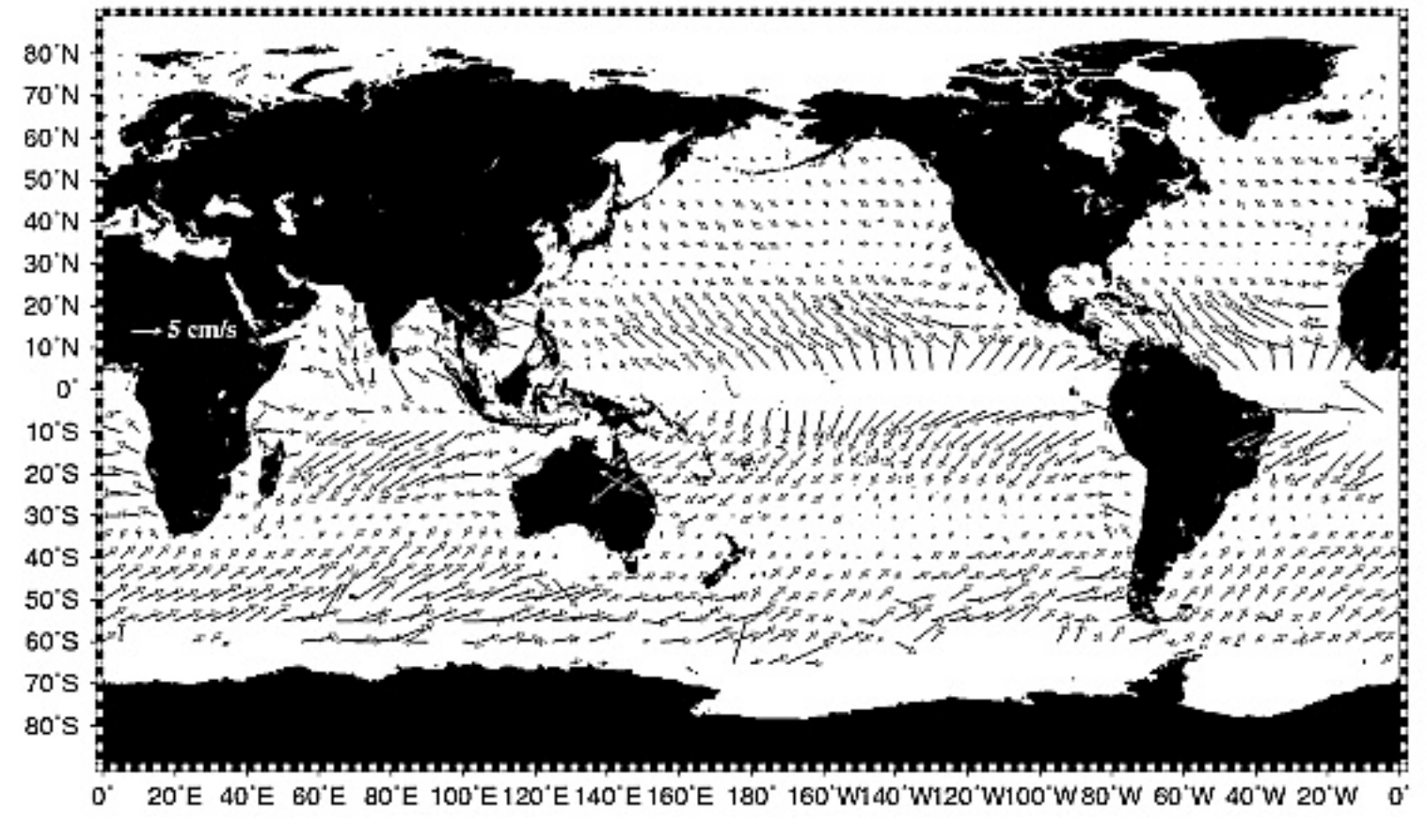


- Two parameter model (angle and amplitude) used to study the response of the upper ocean to wind stress
- Model indicates the current spirals to the right(left) of the winds with depth in the Northern(Southern) Hemisphere
- Model then used to to compute mean and standard deviation of ageostrophic currents
- Mean ageostrophic velocity field shown above
- Large scale features captured
- Strongest flow in equatorial regions with velocities of 5-7 cm/s

# Observing Mesoscale resolution Wind-driven Flow of the California Current

- Methodology is developed to observe mesoscale resolution time-dependent wind-driven ocean velocity estimates
  - Utilization of all data sets available
  - Drifters observations alone are too sparse to observe the mesoscale velocity field
  - Combination of CTD (conductivity, depth, temperature) data with altimetry data to provide estimates of geostrophic current at depth
  - Total flow observations derived from:
    - Satellite tracked drifting buoys
    - Shipboard Acoustic Doppler Current Profilers (ADCP)
    - Maximum Cross-Correlation technique (MCC) applied to 1.1 km Advanced Very-High Resolution Radiometer thermal imagery
- 12-year time series of wind-driven velocity observations is produced (1994-2005) in the California Current System (CCS)
- Regression models, driven by wind velocities from satellite scatterometry and the wind-driven current observations are used to characterize the response of the ocean to wind-forcing

# Ocean Velocity Observations

- Velocity observations are interpolated or composited to 7-day mean velocity fields
  - Minimize the effects of high-frequency ageostrophic currents such as tides and waves
- Geostrophic Currents
  - Combination of satellite altimetry with CTD data to estimate geostrophic currents at depth
- Total Currents
  - Maximum cross-correlation (MCC) technique [Emery 1986; Schmetz and Nuret 1987; Kelly and Strub 1992; Bowen et al. 2002]
    - Feature tracking algorithm that requires minimal user input
    - Simplicity of MCC method, compared to other feature tracking techniques, makes it ideal for the extraction of long time series of velocity data from satellite imagery
  - Drifting Buoys
  - Shipboard ADCP data
    - Gives total current observations at various depths

# California Current System

- California Current System is one of the most thoroughly surveyed regions of the world's oceans
  - North Pacific Current in the northeast Pacific meets the west coast of North America at ~45° N latitude
  - Separates into the poleward Alaskan Current System and the equatorward CCS
  - Comprised of:
    - California Current (equatorward surface current)
    - California Undercurrent (poleward undercurrent)
    - Davidson Current (coastal current)
- Main physical characteristics of the CCS
  - Strong wind forcing
  - Large alongshore scales for wind stress and bottom topography
  - Relatively narrow shelf (width << 10 km) that transitions abruptly offshore to deep basins (depth > 500 m)
  - Coastline from the Baja Peninsula to Oregon is relatively strait, punctuated by large promontories

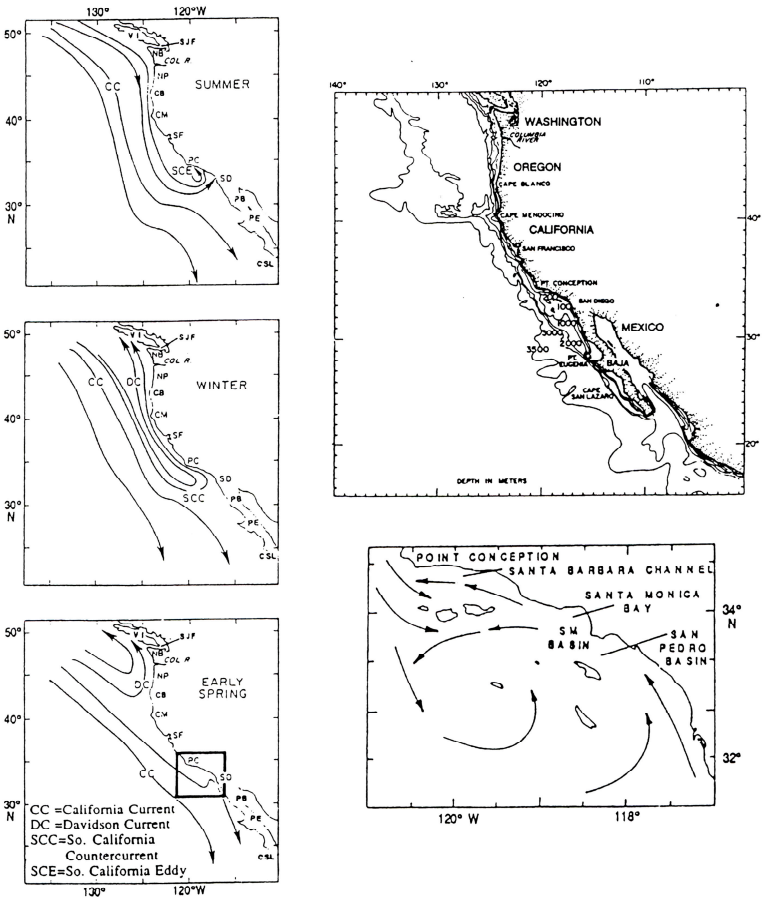

# California Current

- Equatorward surface current
  - Extends ~1000 km offshore
  - Depths of ~500 m
  - Mean speed of ~10 cm/s
- 1970's
  - AVHRR satellite imagery first displayed mesoscale structure
  - Complicated pattern of filaments, meanders, eddies, and jets
- Early 80's
  - Coastal Ocean Dynamics Experiment (CODE) demonstrated energetic eddy and meander field using drifting buoys
  - Patterns agreed with patterns found in imagery

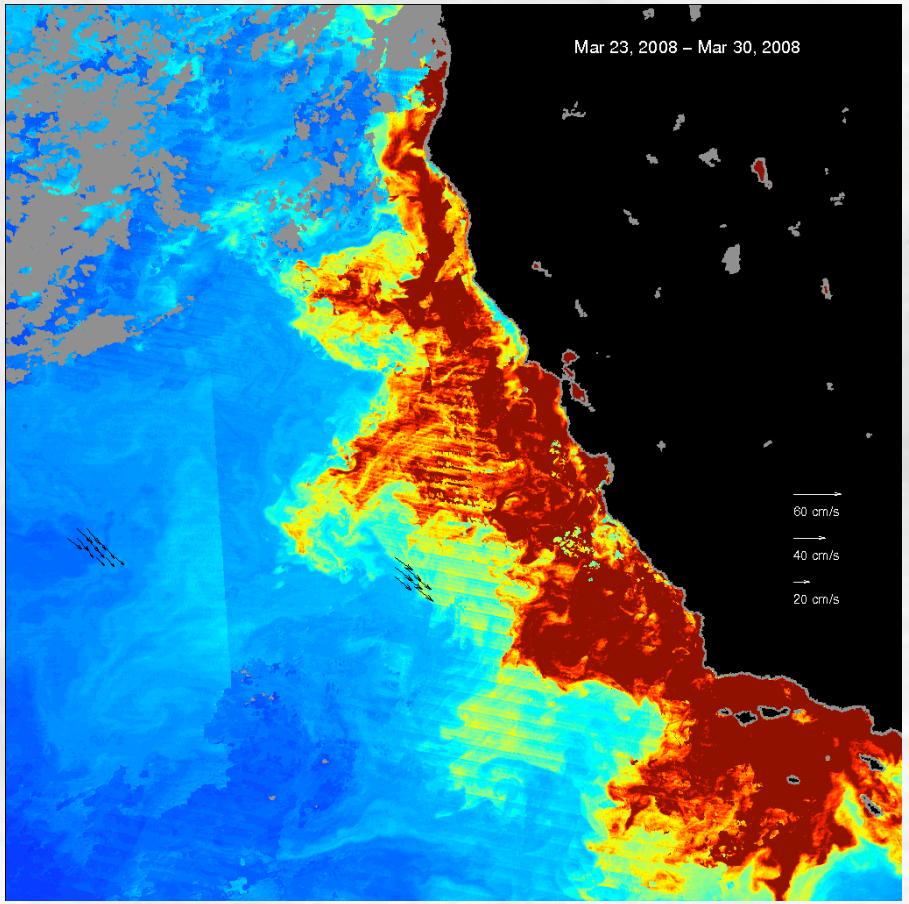

# The Maximum Cross-Correlation (MCC) Method

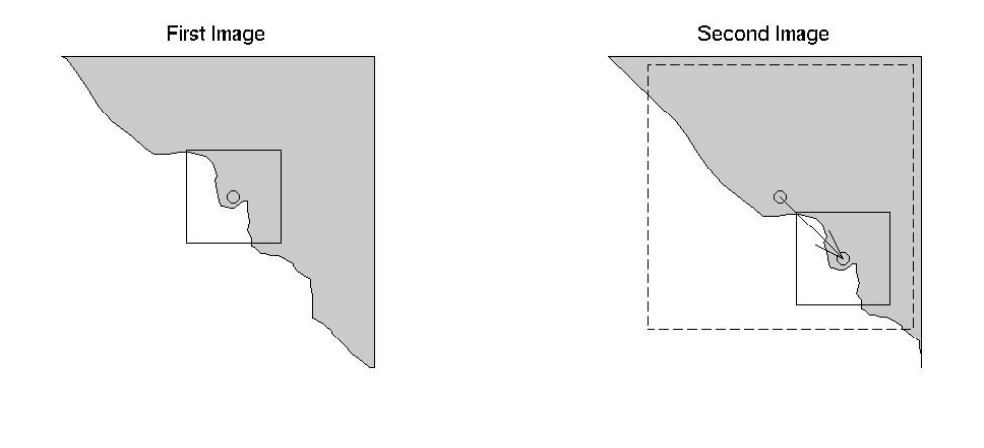


- Automated procedure that calculates the displacement of small regions of patterns from one image to another
- Method has seen variety of tracking applications
  - Cloud motion [Leese et al., 1971]
  - Ice flow [Ninnis et al., 1986]
  - Ocean currents [Emery et al., 1986]
- Method cross-correlates template subwindow in initial image with subwindow of same size in the second image, searching for location, within specified range, that gives the maximum cross-correlation

# MCC Method

- Displacement vector is defined to have its origin at center of initial subwindow and endpoint at center of subwindow in second image that gave the maximum cross-correlation
- Method has two main parameters
  - Size of the template window (solid box in first image)
    - Template window must be large enough to contain multiple independent features that are relate to the number of degrees of freedom, however, must be small enough to resolve the structure of the flow
  - Size of search window (dashed box in second image)
    - Size of the search window is set to accommodate predetermined maximum displacement
- Method serves two purposes
  - Used to precisely navigate AVHRR imagery
  - Estimate ocean currents

# MCC applied to BT Imagery

- AVHRR Imagery
  - Satellite infrared images are obtained from Advanced Very High Resolution Radiometer (AVHRR) on board NOAA 9, 11, 12, 15, and 16 polar orbiting satellites
  - Instrument has a 1.1 km/pixel resolution at nadir
  - Bowen et al (2002) demonstrate more effective to use 11-micron brightness temperature (BT) images compared to computed SST image

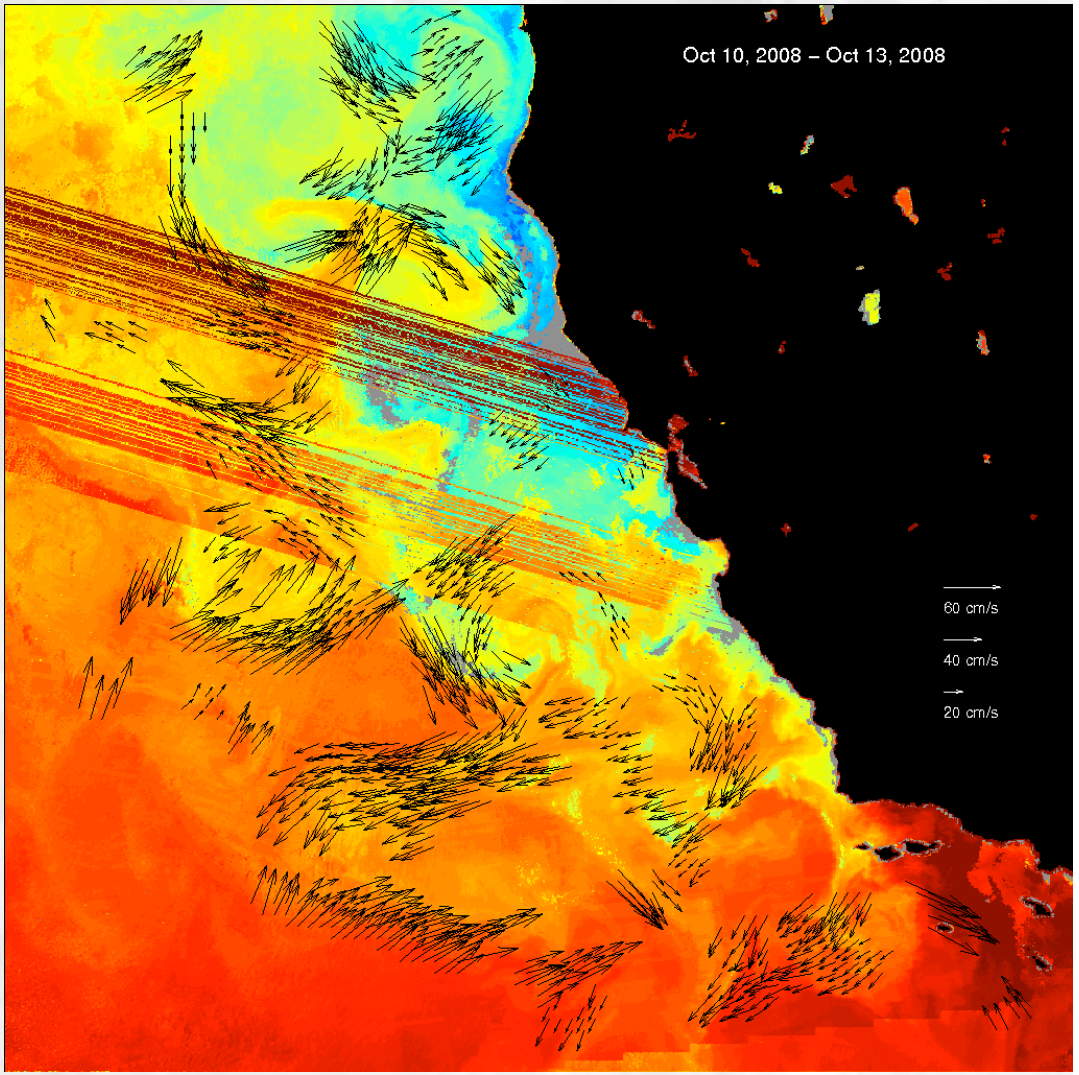

# Image Preparation

- “pre-navigate” the image without any satellite attitude corrections, using only an orbital model and satellite ephemeris data
- MCC method is applied to “base” and target image producing field of land displacement vectors
- “precise image navigation” - combination of geometric image corrections (Earth curvature and rotation) calculated from orbital information, together with georegestration to an accurate map reference, that includes correction for spacecraft timing and attitude errors

# Image Prep.

- Cloud Filter - to obtain quality velocity estimates from AVHRR imagery, clouds must be identified and excluded from consideration
  - Compared to the ocean surface clouds are typically brighter, cooler, and more variable
  - Two thresholds are set:
    - Albedo cutoff: used on daytime channel two (visible) images where pixels brighter than a cutoff are flagged
    - Brightness temperature (BT) threshold, where pixels below 278 K are identified as cloud
  - Temporal Variability Filter:
    - Using the channel 4 images: mean, standard deviation, and max value for each pixel is calculated over the course of ten-day periods
    - Pixel is considered cloudy if its BT is lower than the maximum value minus calculated parameter found using the standard deviation of that pixel over ten days

# MCC Velocity Data

- Method tracks advection of thermal features from one image to the next
- Velocities are found by dividing displacement found by time between images
- Size of search window is set to accommodate predetermined maximum displacement of 100 cm/s
- It was decided that 22 x 22 pixel subwindows consistently gave best representation of the flow based on visual comparisons between several sets of imagery
- Recent study by Crocker et al. [2006] shows no degradation in accuracy for image time separations up to 24 hours (3-24 is used)
- Velocities derived using MCC method are inherently average observations
  - By calculating velocity from displacement of 22 km x 22 km patch of water, an average measurement is made of currents in that patch, over time between images

# MCC Velocity Filter

- Due to automated aspect of this method, vector filtering methodology plays a significant role in the production of accurate ocean velocities
- We find that if a more comprehensive next-neighbor filter is used, correlation cut-off is not required
  - More observations with no reduction in correlation when compared to surface drifter velocities
- Next-neighbor filter
  - Looks at nearest three grid rectangles surrounding vector in question or the 48 nearest points
  - Requiring 10 of those vectors to agree within 10 cm/s magnitude and within 50° direction

# Wind Observations

- Gridded mean wind fields used are from two scatterometer products
- Scatterometers are active microwave sensors: they send out a signal and measure how much of that signal returns after interacting with the target
- The fraction of energy returned to the satellite (backscatter) is a function of wind speed and wind direction
- The wind speed can be determined from the strength of the backscatter signal
- The wind direction is found by the backscatter observed from multiple angles
  - ESA scatterometer AMI-Wind, onboard ERS-1 and ERS-2, is used for time period of 01-1994 to 08-1999
  - For the time period of 09-1999 to 12-2005 weekly gridded wind fields from SeaWinds onboard Quikscat are used

# Geostrophic Velocities Estimates at Depth

- Initial analysis suggested a need to account for vertical geostrophic shear before removing geostrophic signal from total flow products
- Estimates made using any two CTD casts within 80 km and 7 days of each other
- Seasonal means of vertical geostrophic shear for the 12-year study period shown in figure
- Distinct difference is found between upwelling seasons, April to September, and non-upwelling seasons, October to March
- Combining with directions from seasonal mean altimetric velocity fields, spatial mean estimates of geostrophic current at depth are created for each season
- Then applied to 7-day surface MADT velocity fields to produce time-dependent estimates of geostrophic current at specific depths

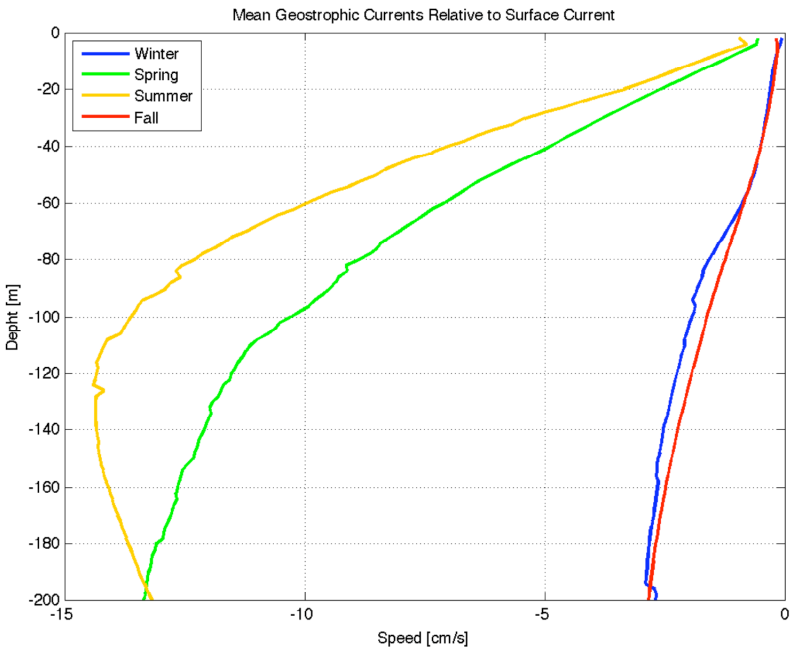

# ADCP Derived Wind Driven Currents

- Necessity to account for geostrophic shear can be seen
- Methodology tested by comparison of deeper observations
- 20 m current demonstrates the largest ageostrophic signal, rotated to right of wind, with a magnitude comparable to surface geostrophic flow
- Residual ageostrophic velocities from 30 to 80 m are all directed to right of wind, consistent with Ekman theory
- Observations demonstrate magnitude and phase decay with depth
- Spiral observed is similar to the Ekman spiral found by Chereskin [1995] that is quantitatively similar to theoretical Ekman spiral, though much flatter in shape

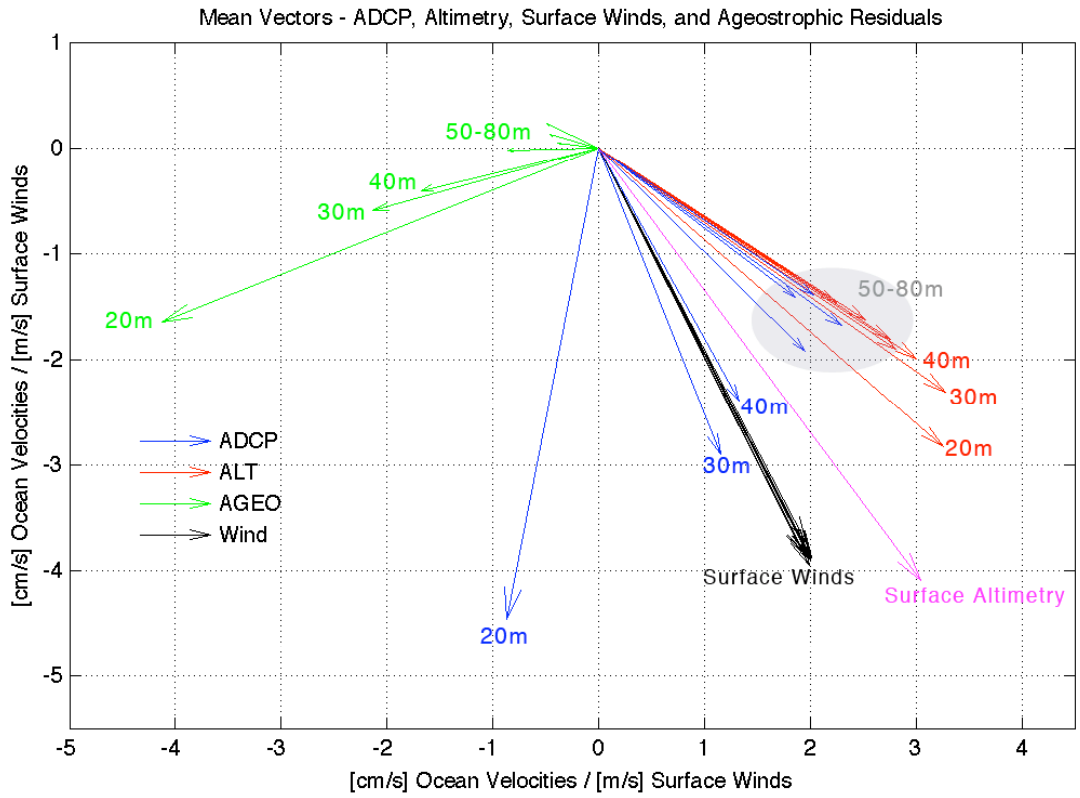

# Depth Estimation of MCC Observations

- To observe mesoscale resolution wind-driven flow, MCC method must be used (drifters alone can not provide enough data points)
- First however, MCC observations depth must to be considered
- By tracking 22 x 22 km patches of water over a time range of 3 to 24 hours, MCC observations are inherently an average observation
- These average velocity measurements are then composited (averaged again) to 7-day velocity fields
- It is hypothesized that through this procedure 7-day composite MCC observations are representative of either some bulk flow or deeper less variable current
- If MCC observations are representative of some depth, characteristic signals should be present when comparing MCC observations against ADCP and drifter velocity estimates
- Also, dramatic differences in the seasonal vertical shear, seen in this region, should vary relationship of MCC observations to ADCP and drifter products
- Through statistical analysis of coincident ADCP and drifter observations, an argument for MCC method, applied to AVHRR images and composited to 7-day fields, producing currents that are representative of flow at some depth is presented

# MCC vs. ADCP

- 400 coincident points for comparison
- Coincident mean MCC and ADCP observations at various depths are shown
- Visual comparison - appears MCC is producing an observation similar to 30 m ADCP

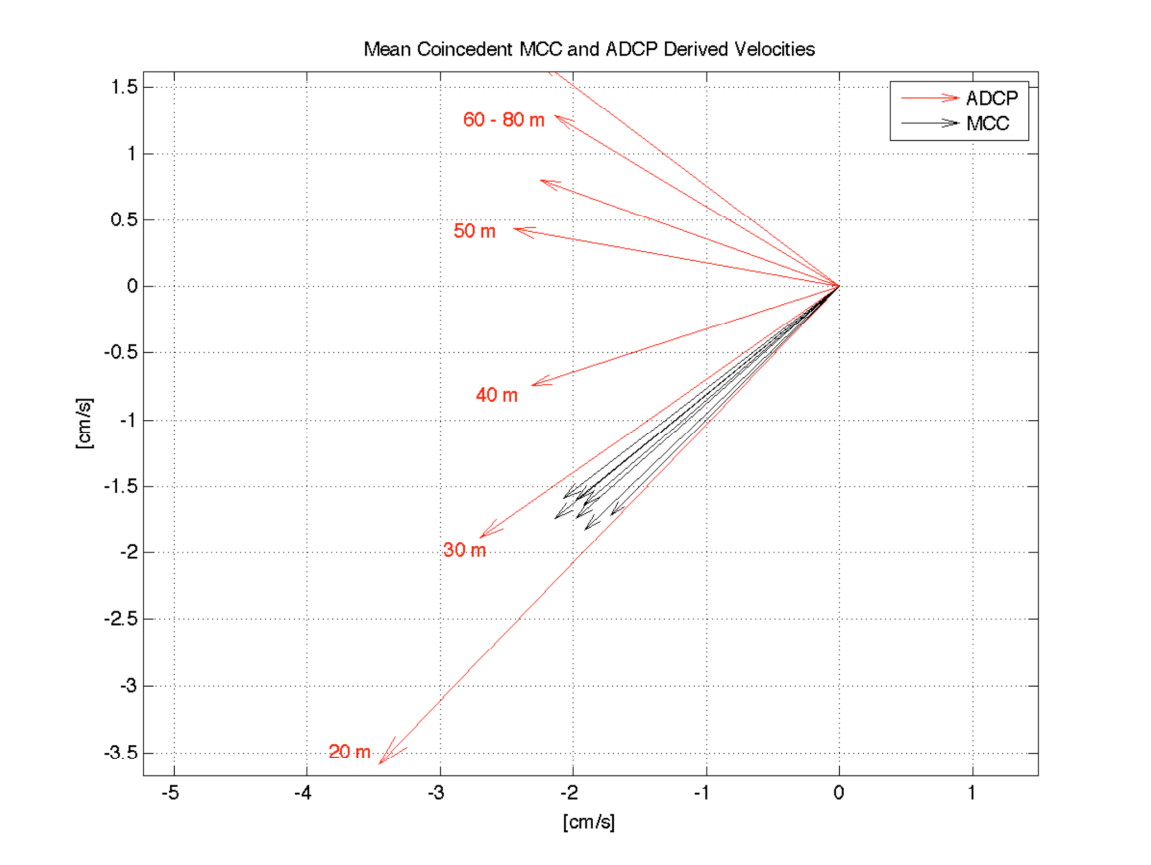

- Rough estimate of possible depth associated with the MCC observations is the “zero-crossing” in bias of magnitude and direction from coincident MCC observations and different ADCP depth observations
- ~30 m zero crossing in directional differences of the current observations
- ~40 m zero crossing in magnitude differences

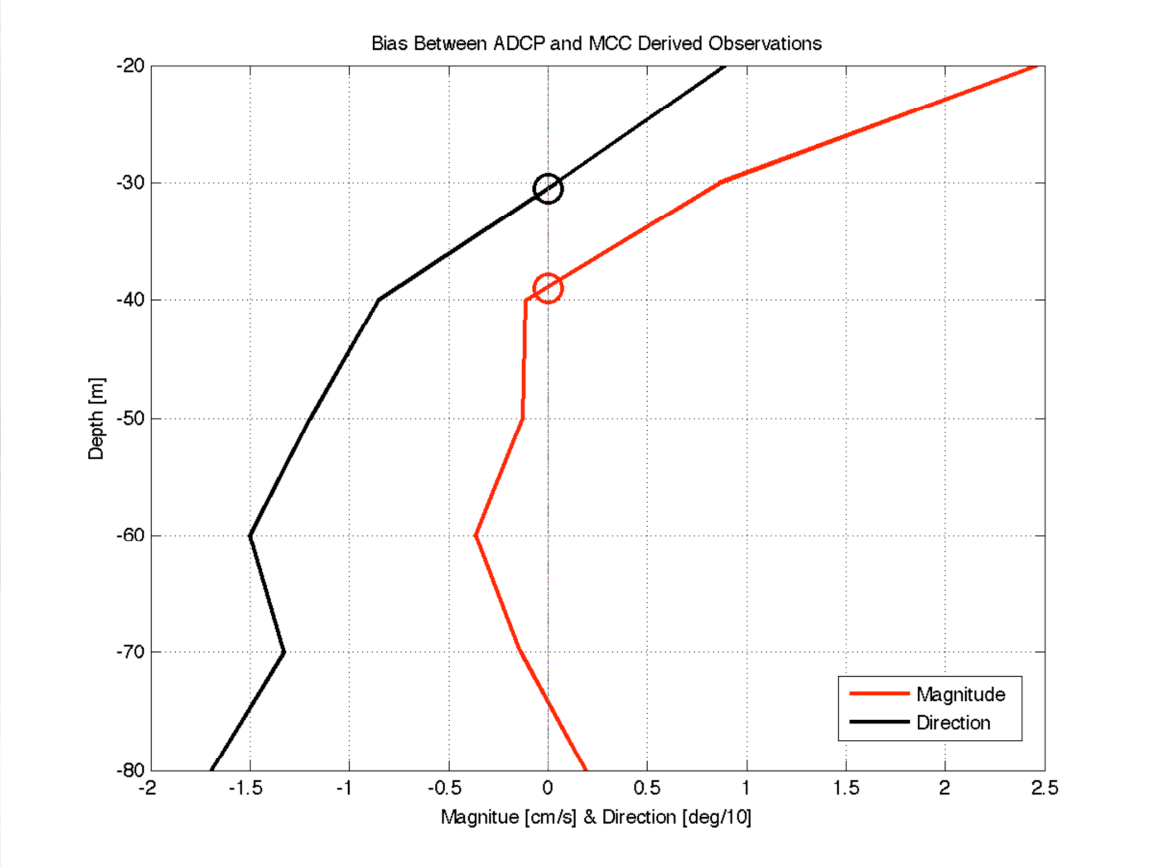

- Correlation coefficients are computed for upwelling seasons, spring and summer, and non-upwelling seasons, fall and winter, independently
- 99% significant levels of agreement only surpassed in upwelling seasons, for depths of 20-40 m
- Suggest MCC observations are most representative of these depths
- Loss of peak and decrease of agreement when shear diminishes does not disprove this result
- During this season, with out any significant shear, any observation of current at any specific depth should display these patterns

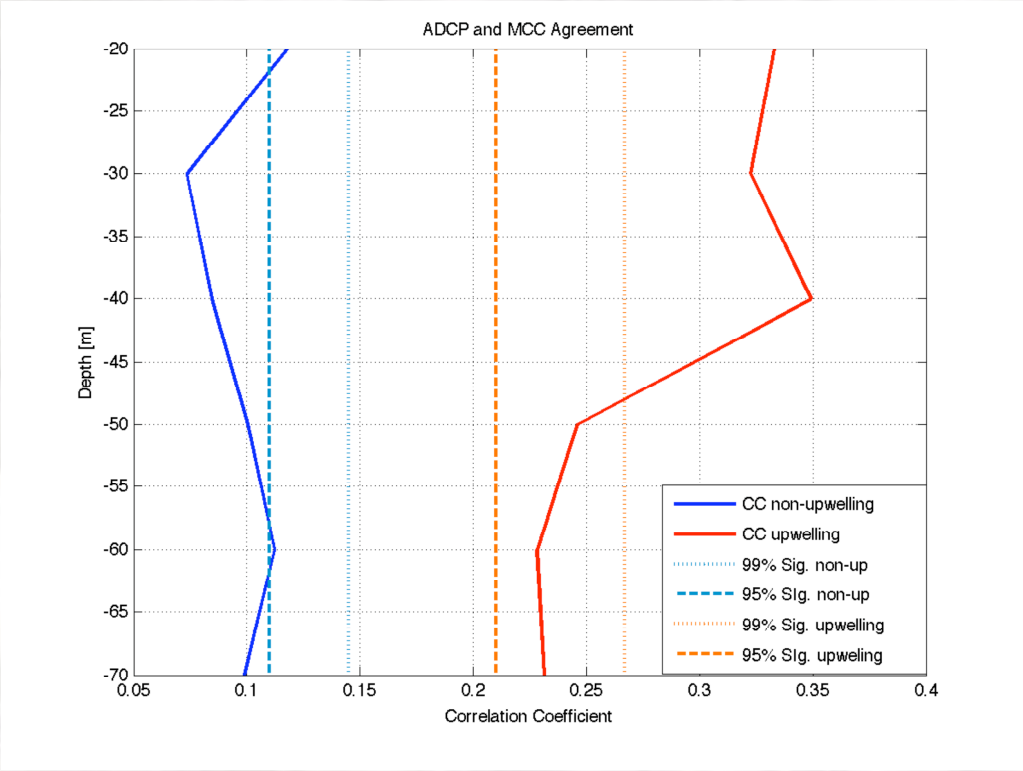

| | Winter | Spring | Summer | Fall |
|---|---|---|---|---|
| Bias – Speed [cm/s] | -1.38 | -6.88 | -7.34 | -3.59 |
| RMS Diff. - Speed [cm/s] | 13.25 | 18.67 | 19.10 | 14.41 |
| Wind Speed [m/s] | 4.8 | 6.3 | 6.4 | 5.1 |

- 2200 coincident drifter and MCC velocity observations available
- Seasonal biases and RMS differences are shown in table
- During upwelling seasons (spring and summer) when wind forcing is larger and vertical velocity shear is dramatic, biases between products are much larger compared to non-upwelling seasons, increasing by a factor of ~3
- RMS differences also show this pattern, increasing from ~14 cm/s to ~19 cm/s

# Choice of Representative Depth for MCC Observations

- When compared to ADCP velocities, MCC observations show mean characteristics that suggest depth of 20-30 m
- When MCC observations are compared to drifter velocities, seasonal differences arise that suggest MCC is measuring a deeper current than the drifter observations
- At very least, it is clear that MCC observations, while measuring surface displacements, are not producing velocities that are characteristic of ocean surface
- 30 m representative depth for MCC observations is assigned
- This choice of depth will be able to be tested by upcoming ageostrophic analysis
- With wind-driven currents showing not only magnitude, but also phase decay with depth, the validity of this 30 m choice will be tested by relationship of MCC ageostrophic product to ADCP and drifter derived ageostrophic products

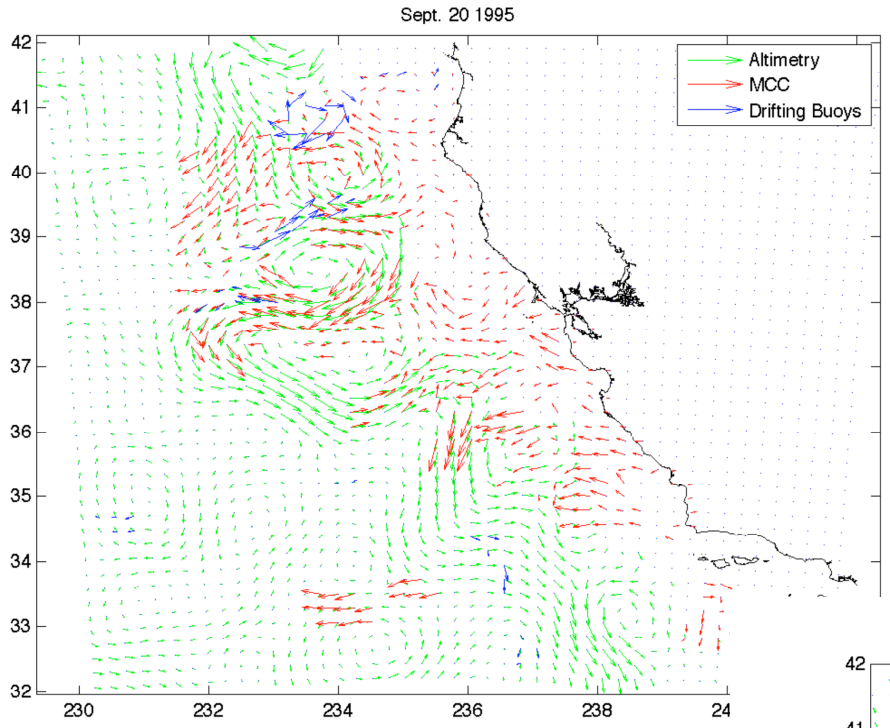


Ocean Velocity Scale

60 cm/s

40 cm/s

20 cm/s

Wind Velocity Scale

20 m/s

10 m/s

5 m/s

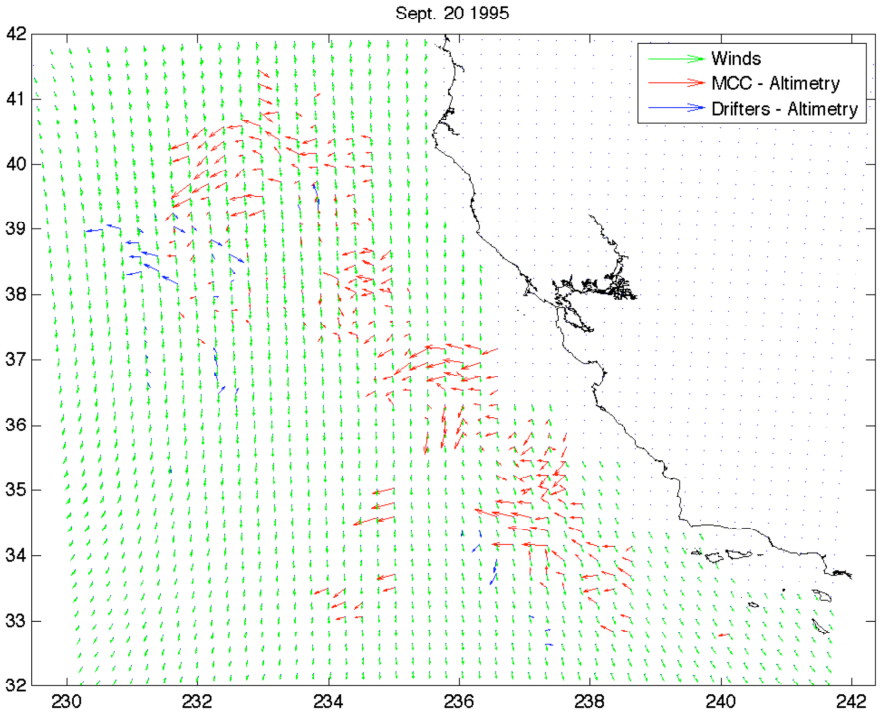

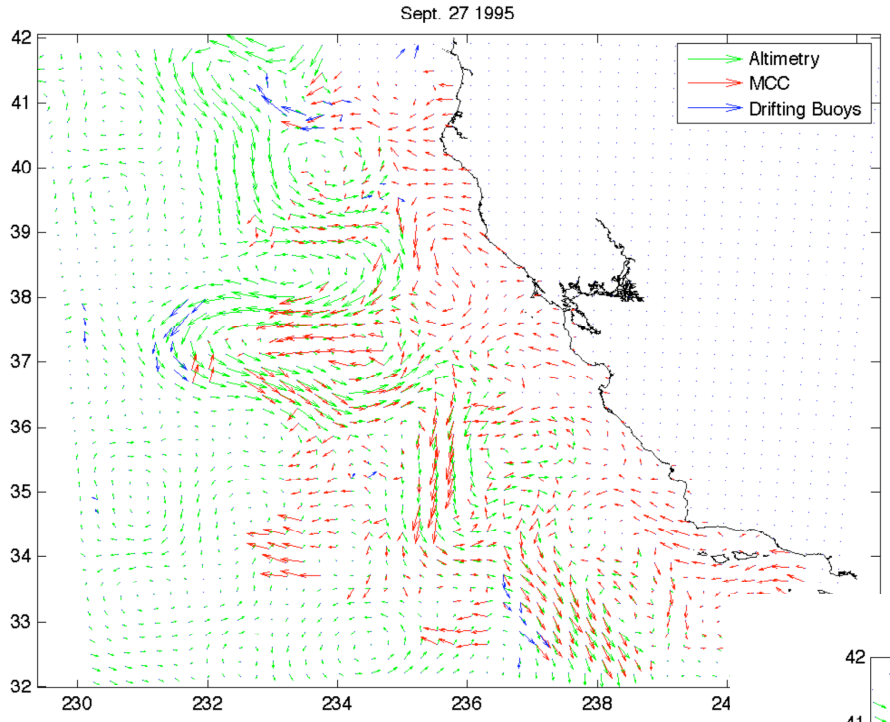
Sept. 27 1995
Altimetry
MCC
Drifting Buoys
42
41
40
39
38
37
36
35
34
33
32
230
232
234
236
238
24





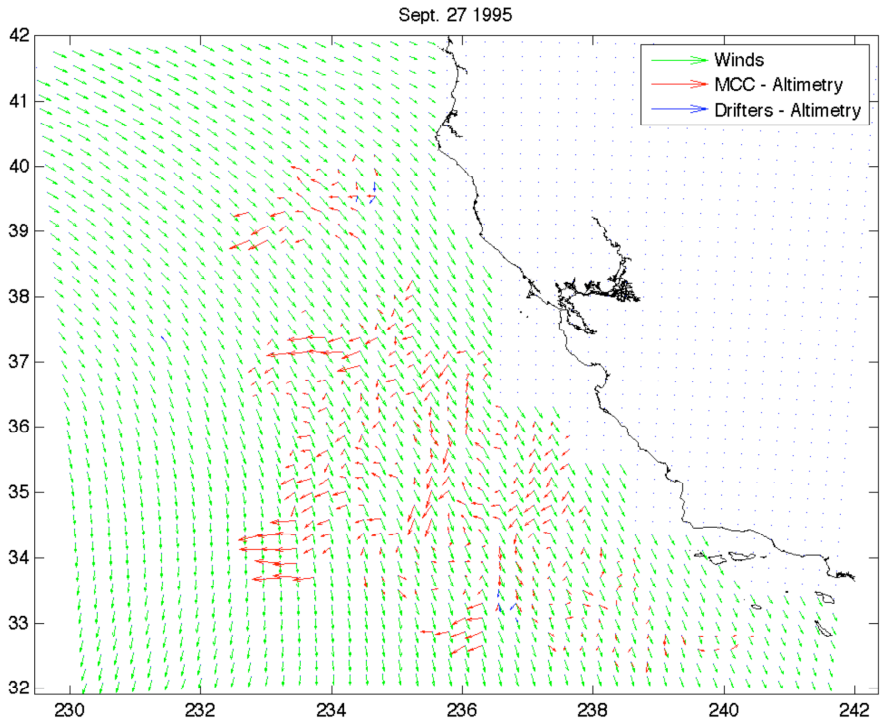
Sept. 27 1995
Winds
MCC - Altimetry
Drifters - Altimetry
42
41
40
39
38
37
36
35
34
33
32
230
232
234
236
238
240
242

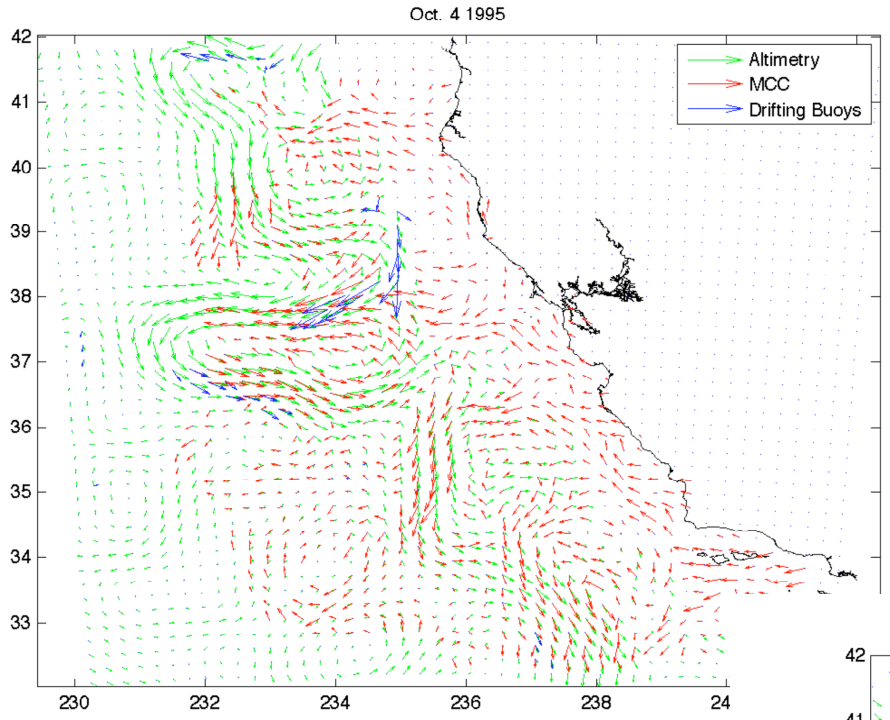
Oct. 4 1995
Altimetry
MCC
Drifting Buoys
42
41
40
39
38
37
36
35
34
33
230
232
234
236
238
24





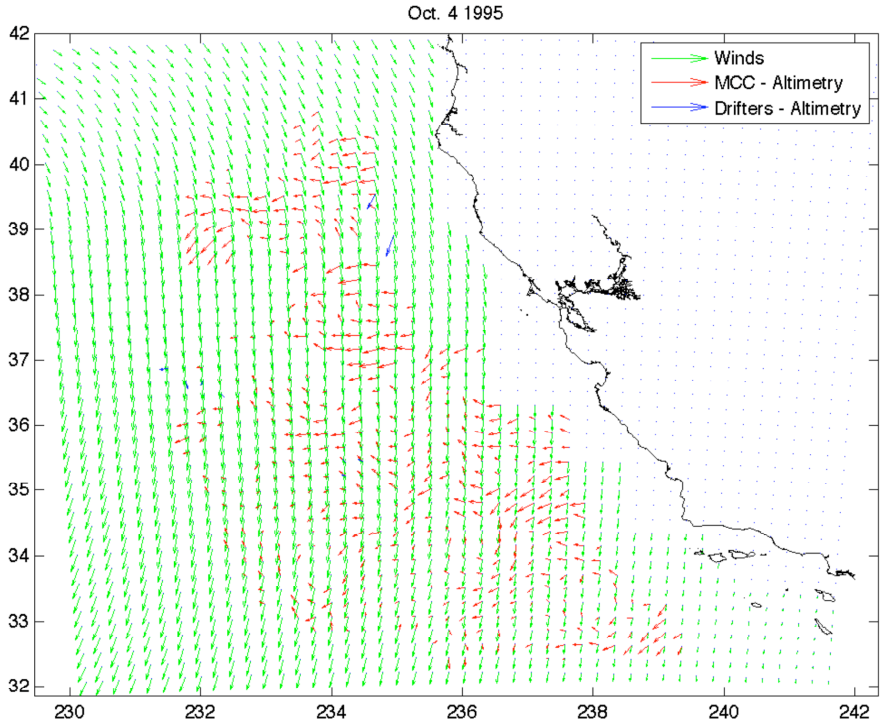
Oct. 4 1995
Winds
MCC - Altimetry
Drifters - Altimetry
42
41
40
39
38
37
36
35
34
33
32
230
232
234
236
238
240
242

# Wind-driven Velocity Statistics

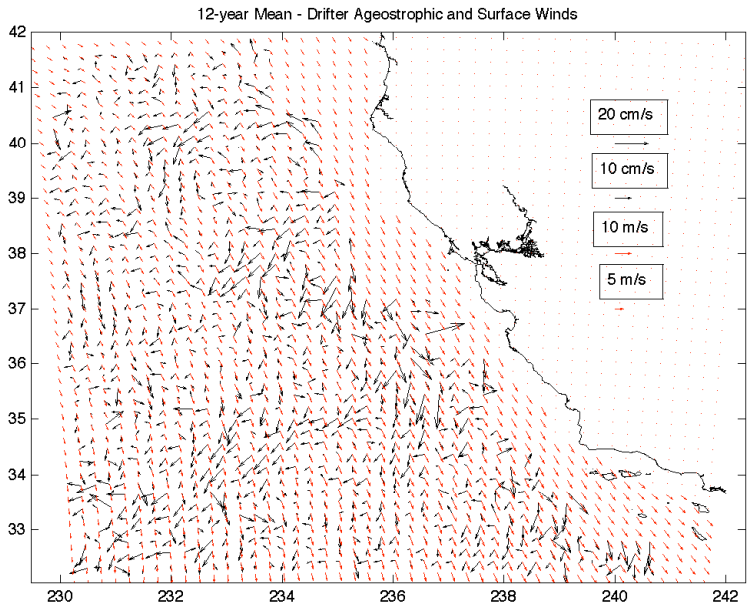


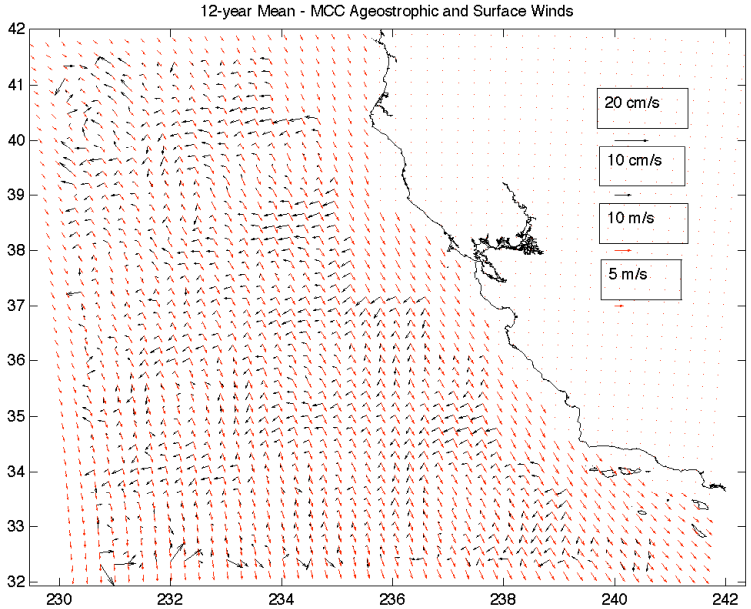


- Fields show ageostrophic velocities that are predominately to the right of the wind with significant spatial structure
- Coastal geostrophic velocities are excluded due to the lower reliability of these data
- Problems with near-shore altimetry observations
  - –Corruption of the return waveform
  - –Corruption of required radiometer wet troposphere correction.
  - –Shorter time and space scales compromise the altimeter measurement precision

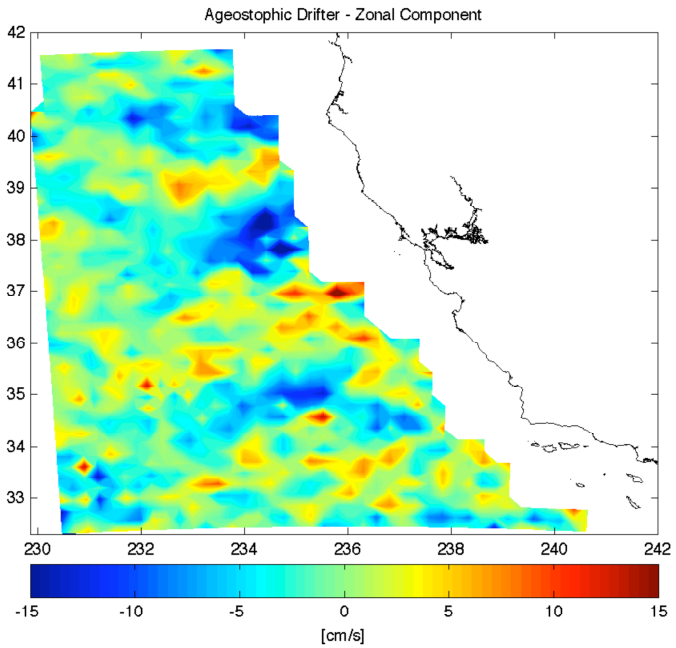


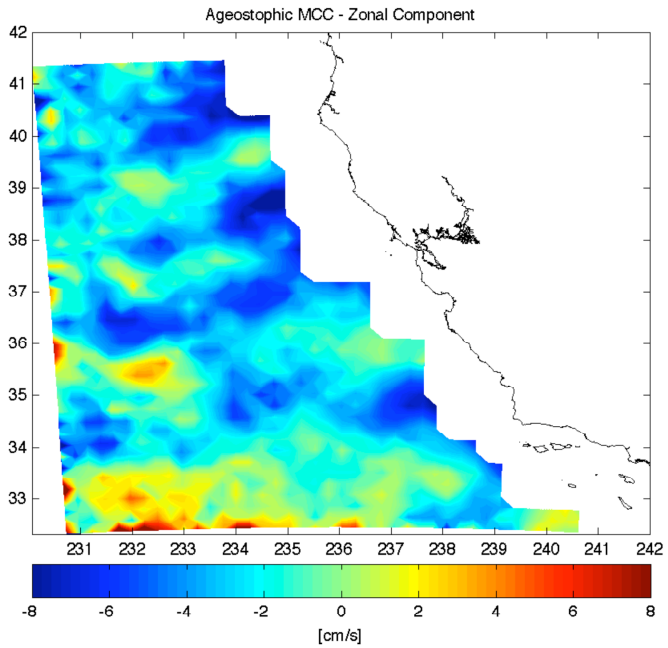


- Mean zonal ageostrophic component for two ageostrophic products
- Patterns are more apparent
- Strong westward offshore flow can be seen in both products at 40° N, 38° N, and 35° N
- Proof patterns not function of MCC observations

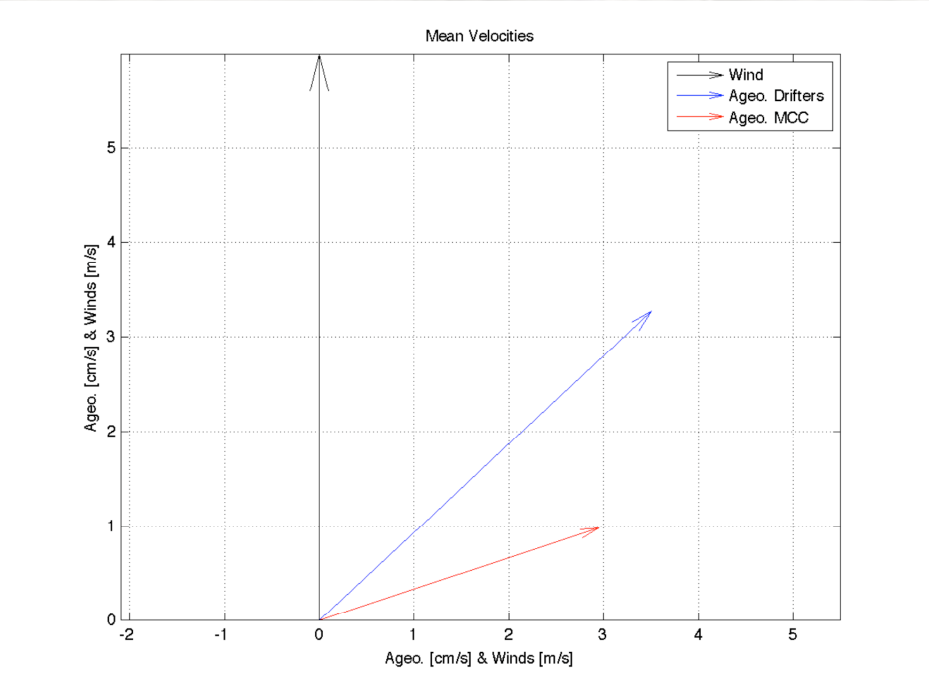


- To quantify average response of ageostrophic observations to wind forcing, we average all ageostrophic currents and coincident winds, to a single vector for each product
- Then rotate wind to due north and rotate ageostrophic currents relative to wind
- Scale is applied mean ageostrophic vectors, relative to strength of coincident wind
- If assumed MCC depth of 30 m is valid then methodology and observations are producing an Ekman-like response
- 15 m drifters and assumed 30 m MCC ageostrophic currents show magnitude and phase decay with depth

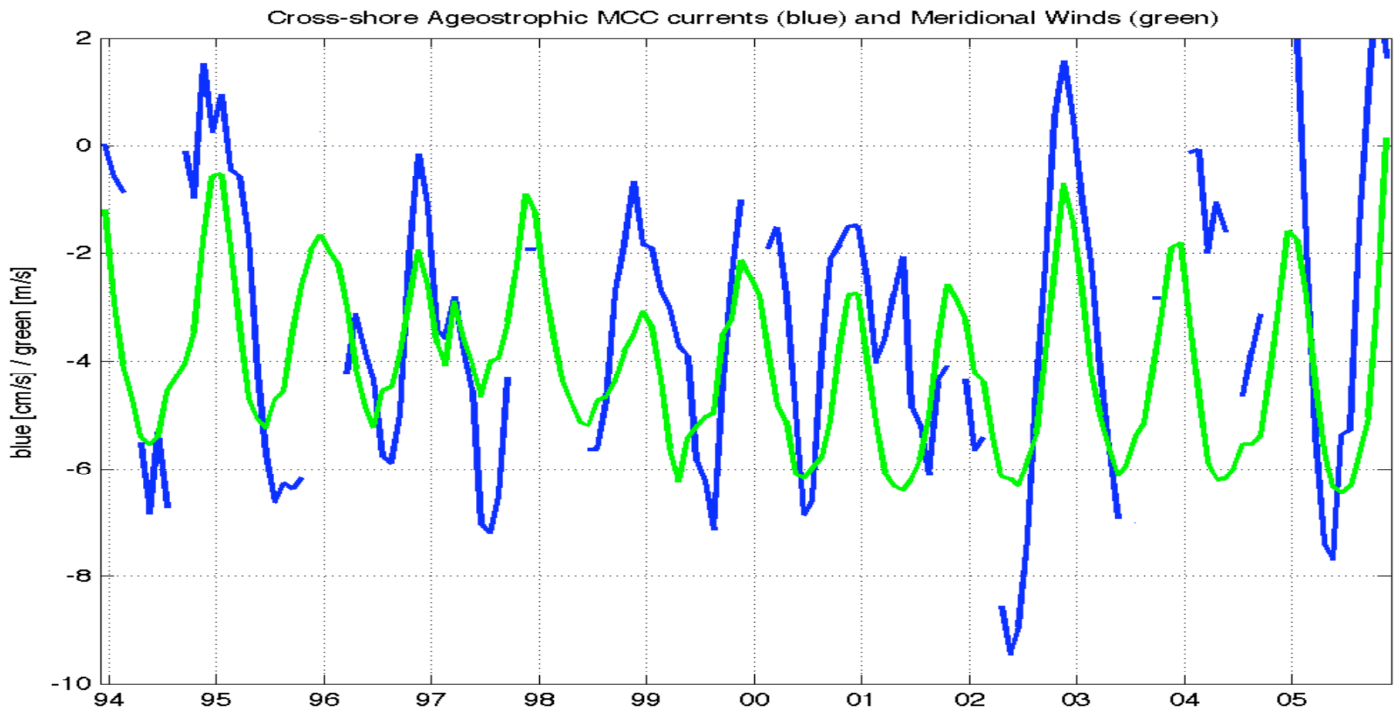


- Time series of monthly ensemble average wind and current measurements. The series show the temporal evolution of the cross-shore ageostrophic currents from MCC and meridional winds from scatterometry
- Correlation Coefficient of 0.68 significant at 99% level

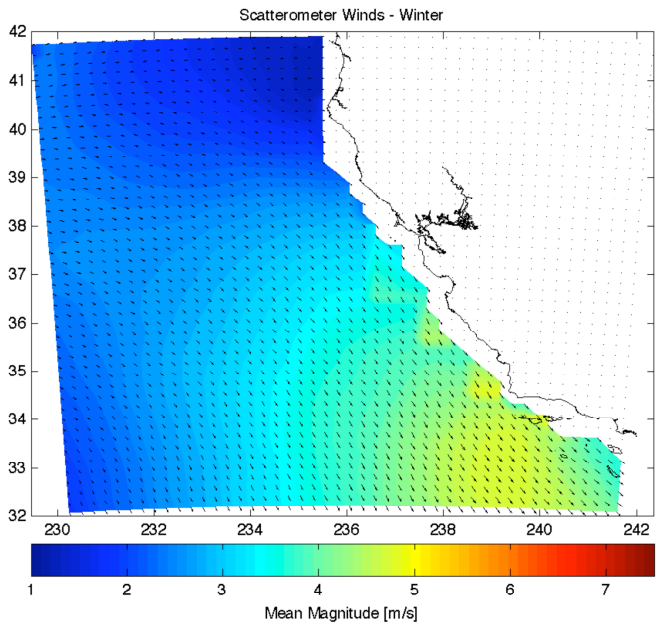
Scatterometer Winds - Winter
42
41
40
39
38
37
36
35
34
33
32
230
232
234
236
238
240
242
1
2
3
4
5
6
7
Mean Magnitude [m/s]

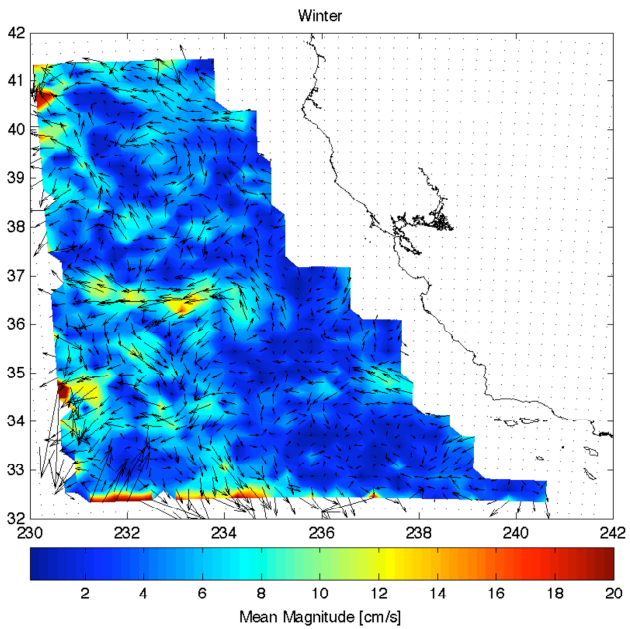
Winter
42
41
40
39
38
37
36
35
34
33
32
230
232
234
236
238
240
242
2
4
6
8
10
12
14
16
18
20
Mean Magnitude [cm/s]

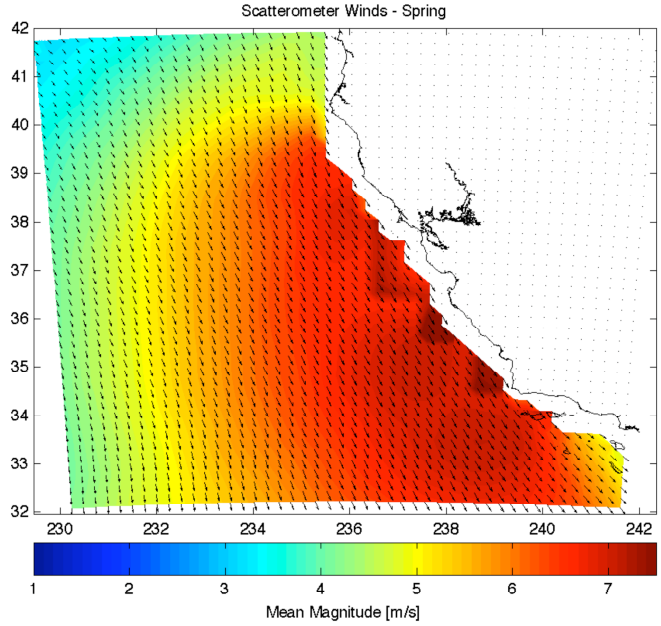
Scatterometer Winds - Spring
42
41
40
39
38
37
36
35
34
33
32
230
232
234
236
238
240
242
1
2
3
4
5
6
7
Mean Magnitude [m/s]

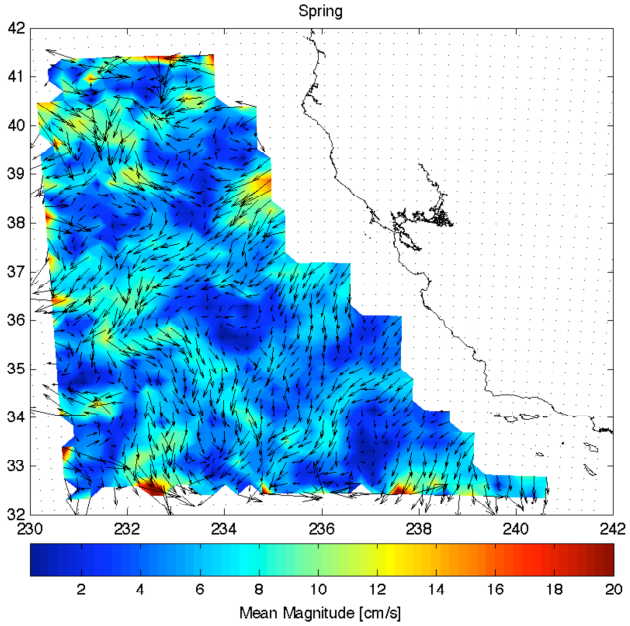
Spring
42
41
40
39
38
37
36
35
34
33
32
230
232
234
236
238
240
242
2
4
6
8
10
12
14
16
18
20
Mean Magnitude [cm/s]

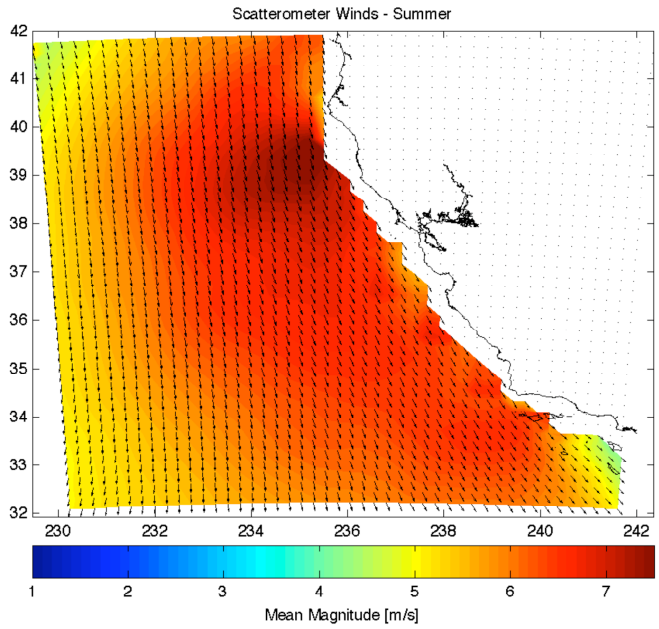
Scatterometer Winds - Summer
42
41
40
39
38
37
36
35
34
33
32
230
232
234
236
238
240
242
1
2
3
4
5
6
7
Mean Magnitude [m/s]

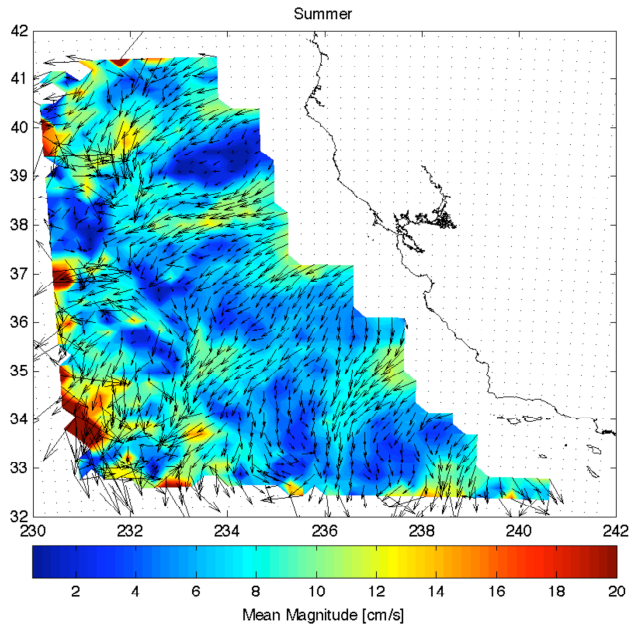
Summer
42
41
40
39
38
37
36
35
34
33
32
230
232
234
236
238
240
242
2
4
6
8
10
12
14
16
18
20
Mean Magnitude [cm/s]

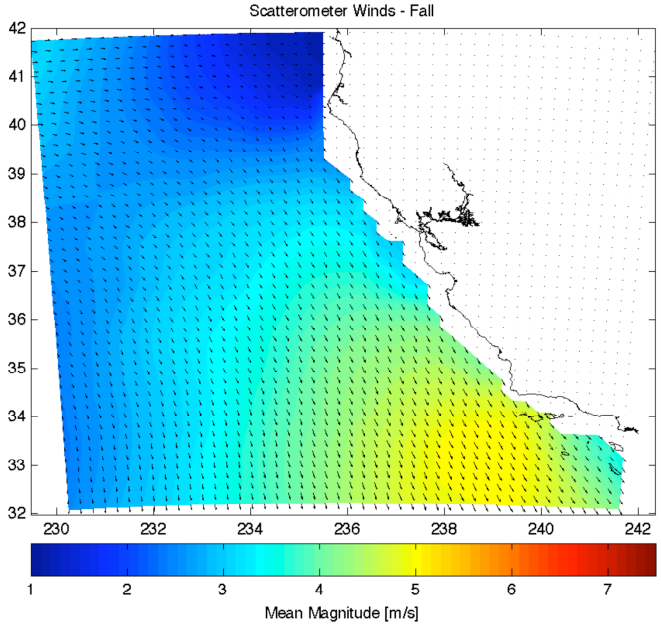
Scatterometer Winds - Fall
42
41
40
39
38
37
36
35
34
33
32
230
232
234
236
238
240
242
1
2
3
4
5
6
7
Mean Magnitude [m/s]

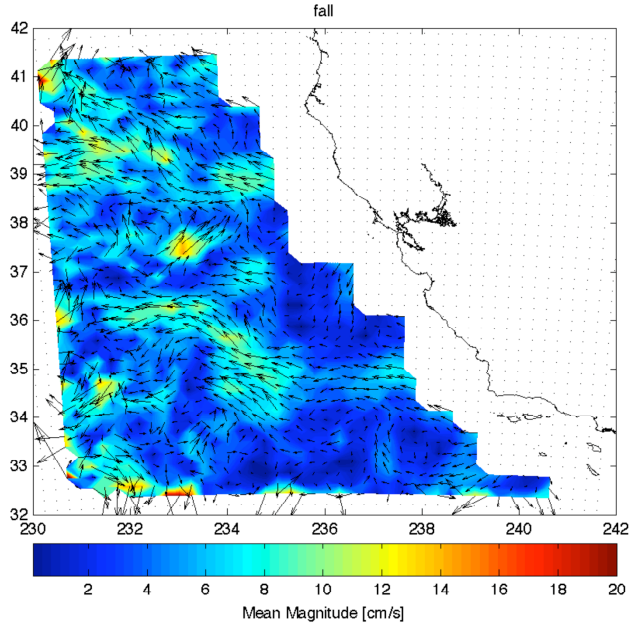
fall
42
41
40
39
38
37
36
35
34
33
32
230
232
234
236
238
240
242
2
4
6
8
10
12
14
16
18
20
Mean Magnitude [cm/s]

# Regression Models

- To study response of wind-driven currents to ocean surface winds, two separate regression models are used
- First model
  - Depth independent
  - Used to determine the vertical structure of the Ekman dynamics by considering each ageostrophic data set independently (note that MCC and drifter derived observations, and the ADCP derived observations, at each different observation depth, are each considered a separate ageostrophic data set)
- Second model
  - Assumes constant vertical turbulent viscosity
  - Allows this model to account for the depth of observation
  - Enables model to use of all ageostrophic “products” to determine horizontal characteristics of ocean response to wind forcing

# Model 1 - Vertical Response

- First regression model based on assumption that response of wind-driven current to wind stress is linear [Niiler and Paduan 1995, Van Meurs and Niiler 1996]
- Where β is amplitude relating wind-driven currents to surface winds
- θ is angle between wind and ocean current, with negative angles indicating a current rotated clockwise from wind direction.
- The variables β and θ are estimated using linear least squares techniques that find parameter values that minimize the square difference between model and observations

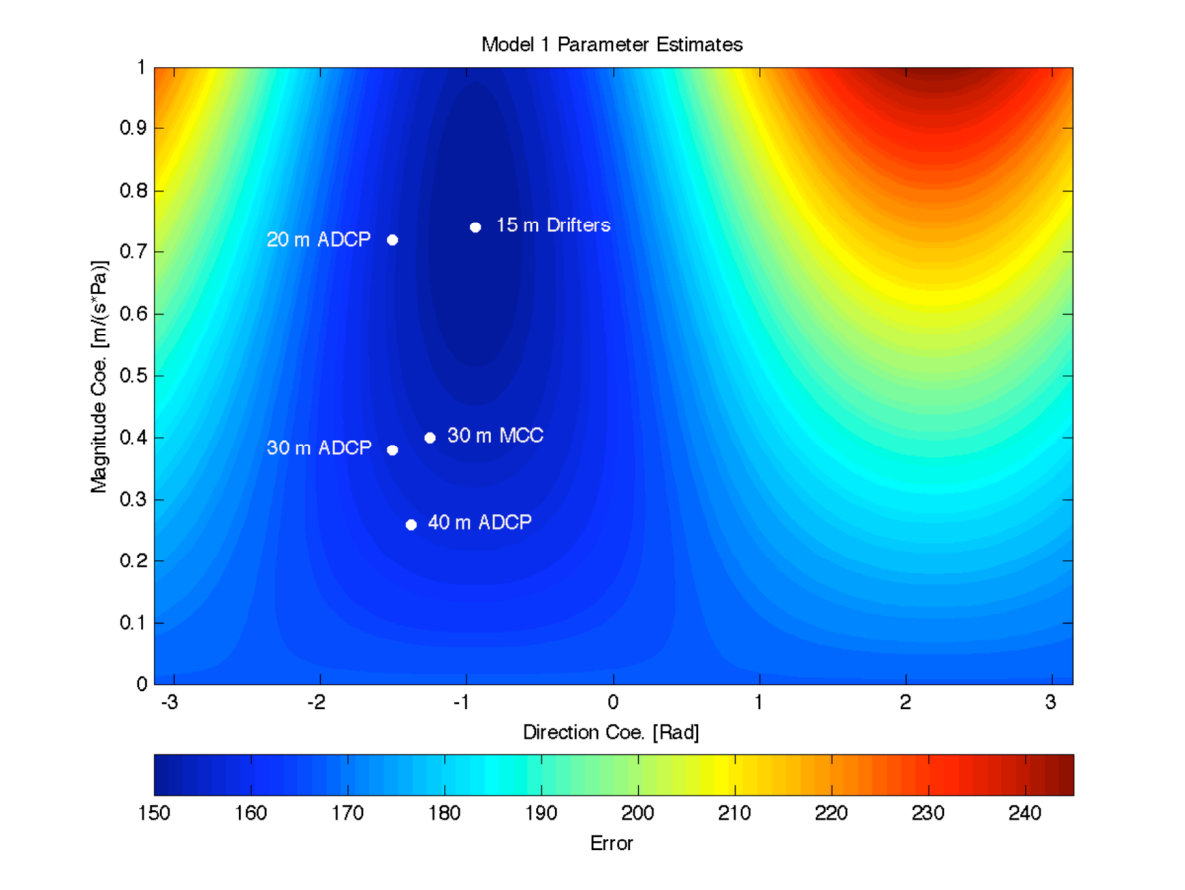


$$u_E + iv_E = \beta C_D \rho_a e^{i\theta} \left| u_W + iv_W \right| \left( u_W + iv_W \right)$$

- Location of magnitude and direction parameters that give the global minimum values of error between wind stress and different ageostrophic products as function of depth
- Similarity of parameters estimated from 30 m ADCP and assumed 30 m MCC ageostrophic products suggest that hypothesized representative depth of MCC observations is valid
- Magnitude parameters show strong linear response
- Drifter, MCC, and 40 m ADCP parameters do demonstrate spiral shape consistent with Ekman theory

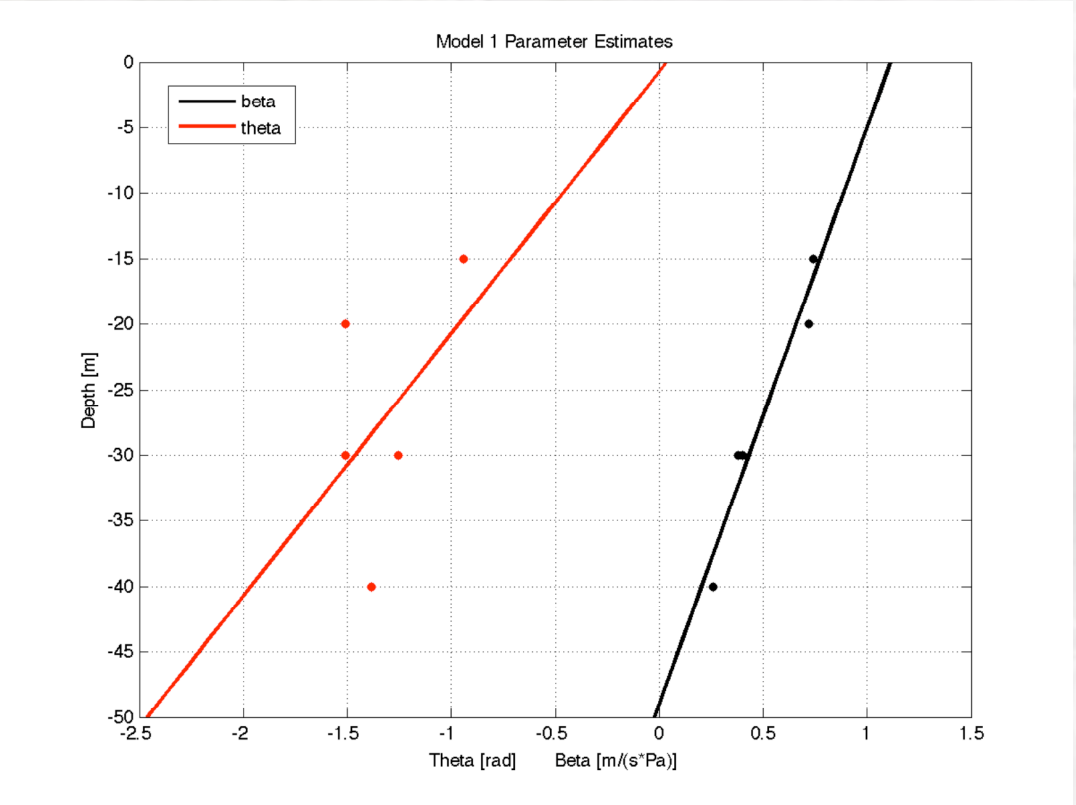

# Model 2 - Horizontal Response

- Model assumes constant turbulent viscosity
- $V_0$ is total Ekman surface current
- $D_E$ is effective depth of Ekman layer, or depth of flow where current is in an opposite direction of surface
- Regression model estimates parameters $\alpha$ and $D_E$ using linear least squares regression
- Model takes into account depth of observation, regression is run on all of ageostrophic velocity observations from various data sets at different depths

$$A_v = \frac{D_E^2 f}{2\pi^2} \qquad V_O = \frac{\alpha U_W}{\sqrt{\sin(\varphi)}}$$

$$u_E = \pm V_0 \cos\left(\frac{\pi}{4} + \frac{\pi}{D_E} z\right) \exp\left(\frac{\pi}{D_E} z\right)$$

$$v_E = V_0 \sin\left(\frac{\pi}{4} + \frac{\pi}{D_E} z\right) \exp\left(\frac{\pi}{D_E} z\right)$$

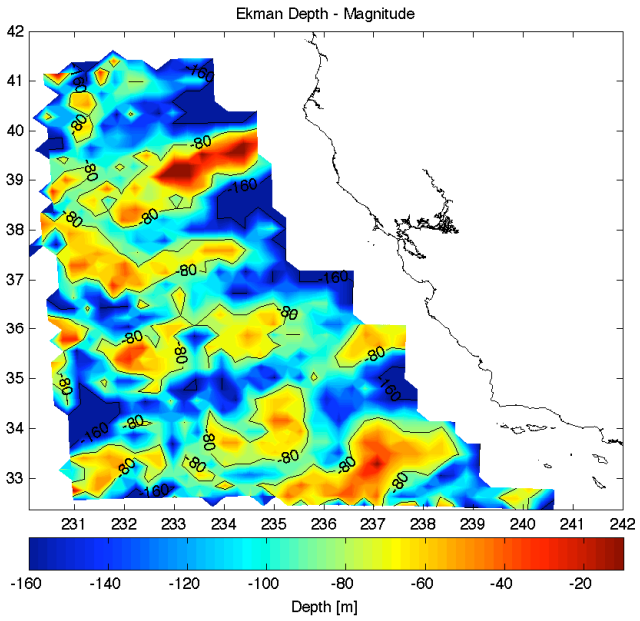


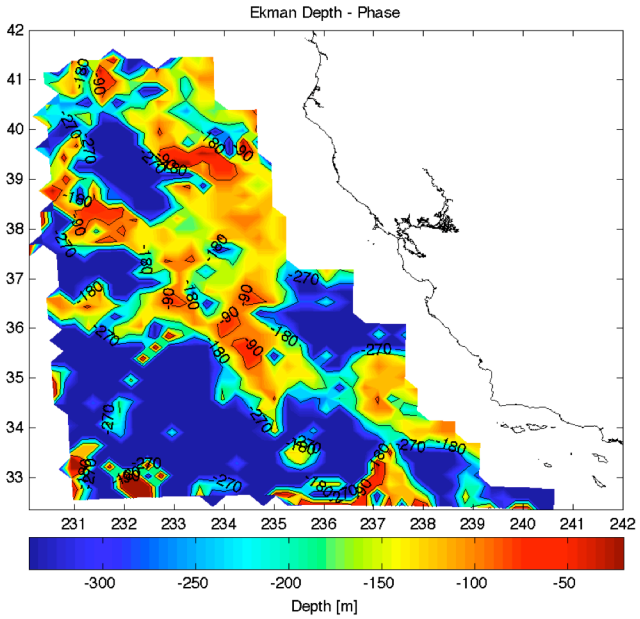


- The model was found to only give reasonable values if estimates are made for $D_E$ parameters in Ekman solution separately
- Minimum is found for phase decay controlling depth and for magnitude decay controlling depth, independently
- Weller [1981] and Chereskin [1995] both observed spirals that were flatter in shape compared to theoretical spiral, leading each to estimate viscosities based on amplitude decay and rotation rate independently
- Global parameters estimated agree with previous studies
- Spatial distributions of Ekman depths are solved for using global $\alpha$ parameter estimate
- Deeper filaments in magnitude map indicate where frictional influence of wind is higher
- Deep values in phase map indicate where geostrophic observations demonstrate little rotation with depth

- Ekman proposed that vertical turbulent viscosity parameter (that controls frictional influence of the wind) is proportional to square of wind speed
- Several other studies have suggested this
- May be true for open ocean wind-driven currents, but not what is found here

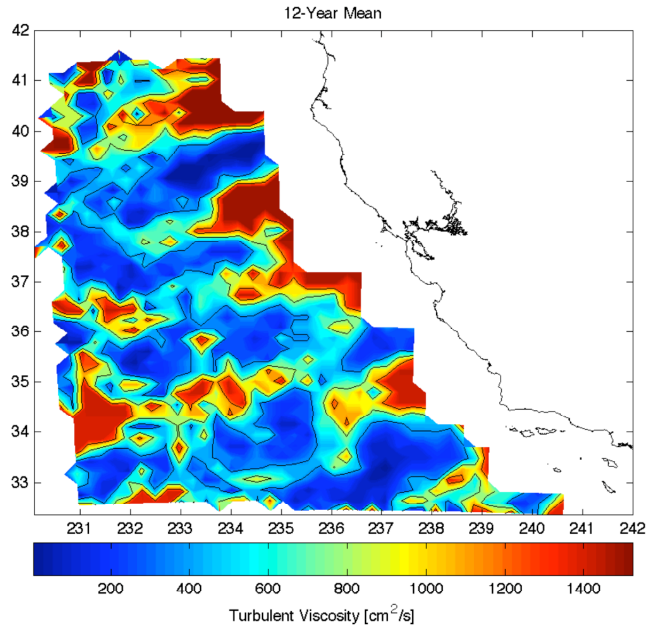


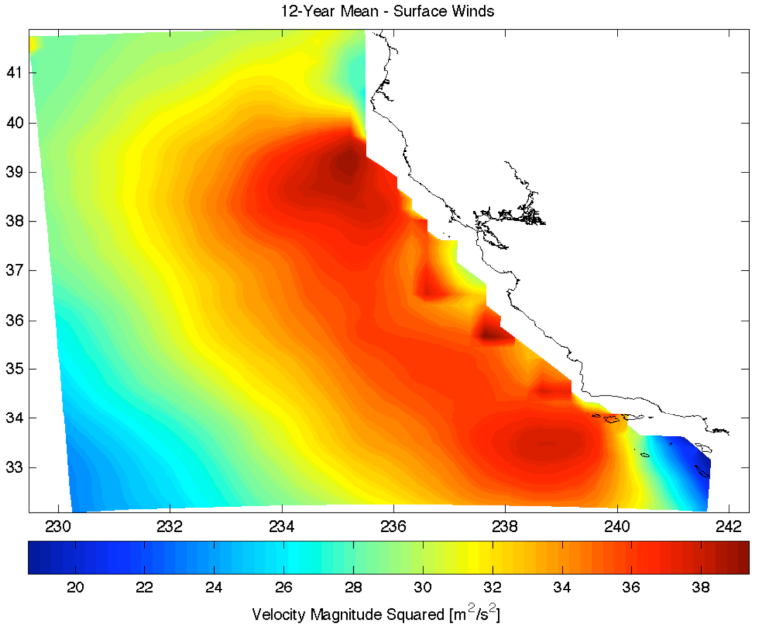

- Two example summertime AVHRR brightness temperature images, along with mean summer turbulent viscosity and wind divergence
- Strong visual correlation between location of SST fronts, patterns of wind divergence, and increased wind-driven activity
- After further analysis this idea was abandoned
- It is believed, though, that stronger wind-driven influence in these regions leads to increased upwelling, and that this upwelling creates strong SST gradients that are driving the wind divergence patterns seen

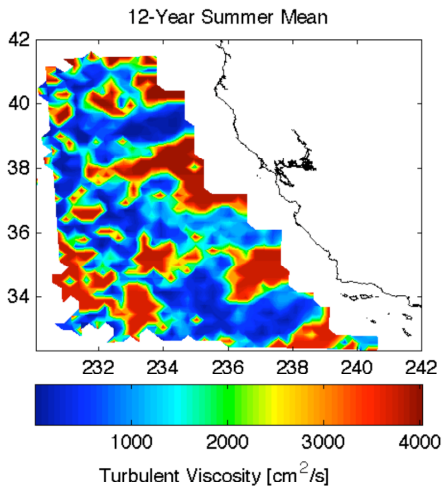


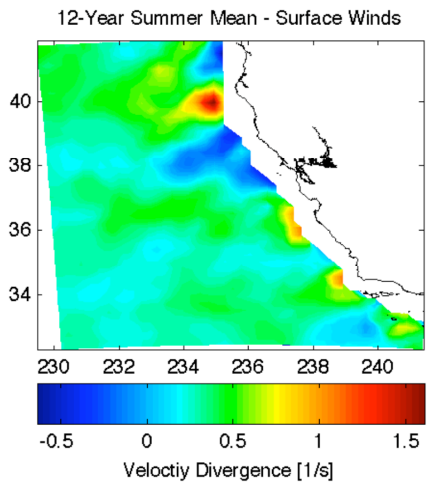


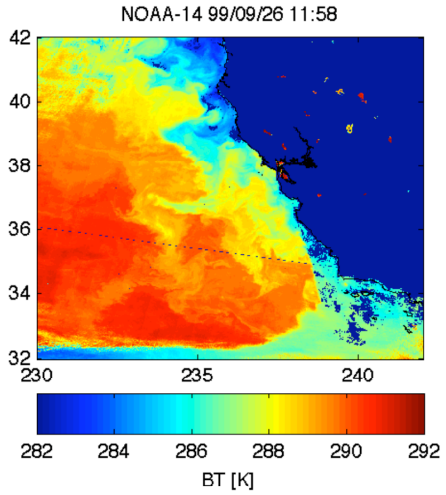


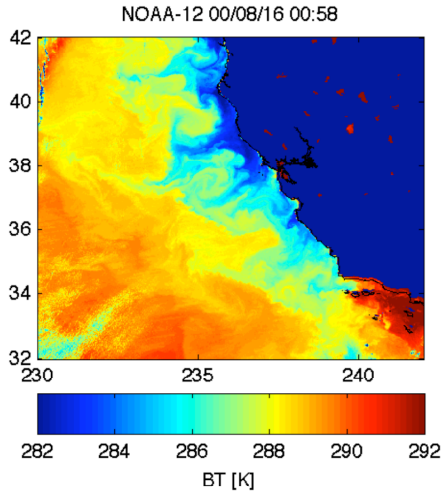

Maximenko et al. 2008

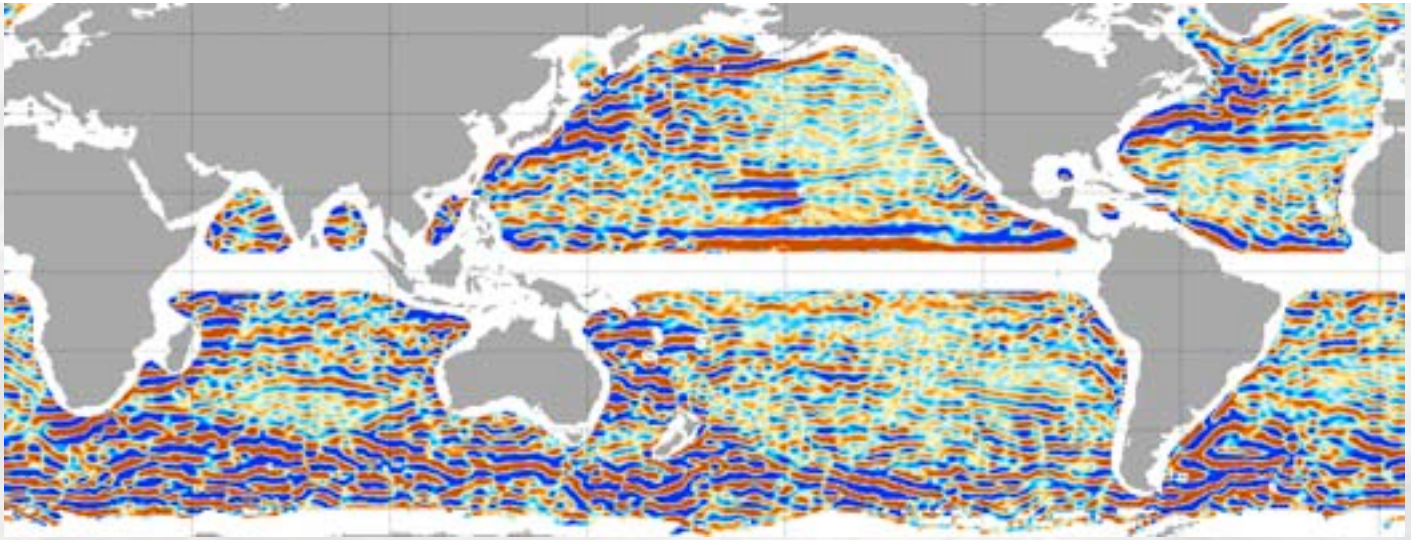

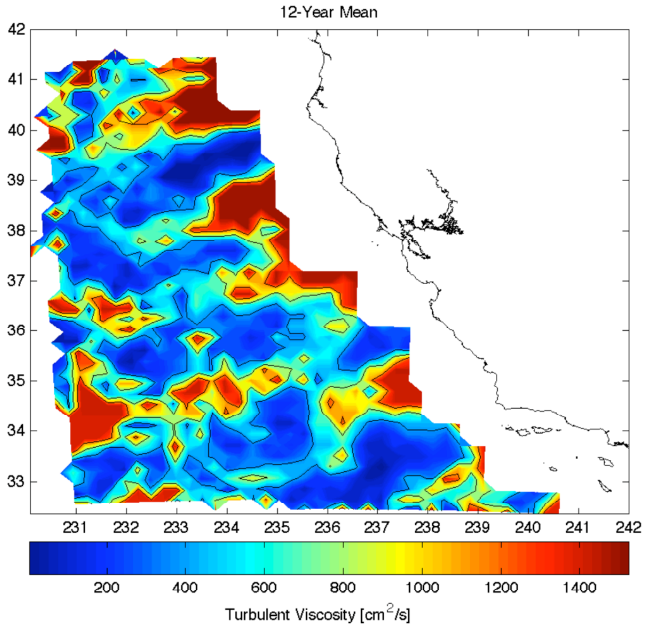


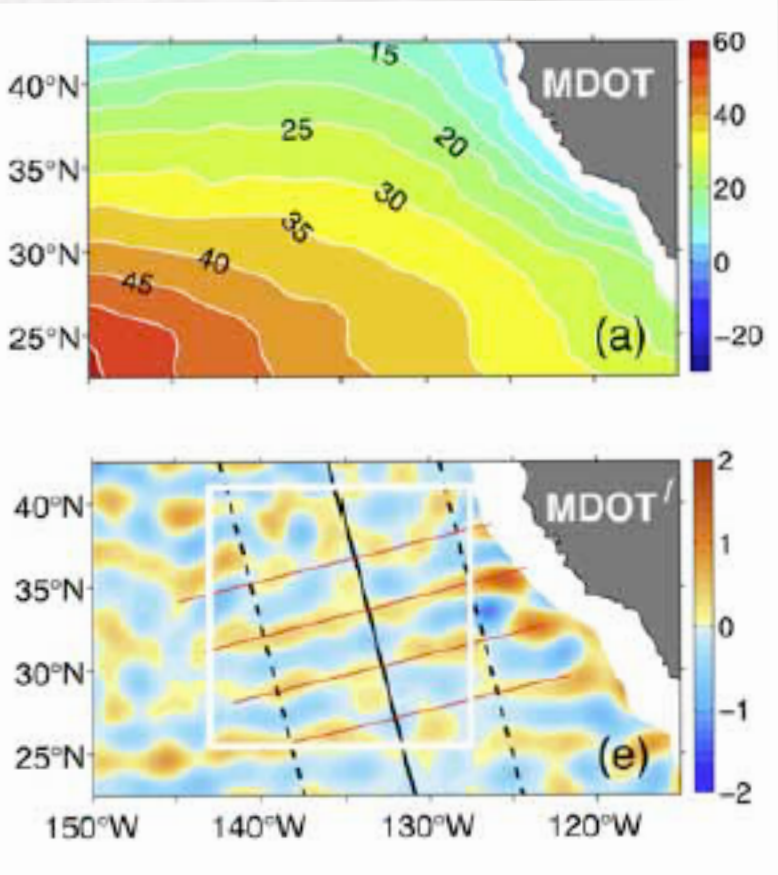

# Conclusions and Discussion

- 12-year time-series of wind-drive currents for California Current region is produced
- Demonstrate strong seasonal response to winds
- Regression models:
  - Demonstrate strong linear vertical ocean response
  - Horizontal response demonstrate regions of increased wind influence offshore of major coastal promontories, unaffected by spatial distribution of wind speed
- Regions of increased wind-driven flow are directly tied to shape of coastline
  - Seen by by near-shore forcing characteristics extending much farther offshore of these features
- Same regions coincide with:
  - Areas of cold core filament production
  - Meanders in the along-shore flow are commonly seen
  - Divergence patterns in wind fields